ANALYSIS GUIDE FOR VARIABLE FREQUENCY DRIVE OPERATED CENTRIFUGAL PUMPS

by

Thomas F. Kaiser

Lead Engineering Analyst

Sulzer Pumps (US) Inc.

Portland, Oregon

Richard H. Osman

Principal Product Engineer

Siemens LD-A

Pittsburgh, Pennsylvania

and

Ralph O. Dickau

Senior Engineering Specialist

Enbridge Pipelines

Edmonton, Alberta, Canada

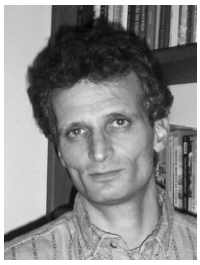

Thomas F. Kaiser has been an Engineering Analyst with Sulzer Pumps (US) Inc., in Portland, Oregon since 1996, leading the analysis team since 2001. In this position he is responsible for performing stress, finite element, rotordynamic, and vibration analyses for new and installed centrifugal pump applications, calculation tool development, and seismic qualification analyses. He began his career in 1994 with Sulzer Pumps Headquarters in Winterthur, Switzerland, as a development engineer working in the field of rotordynamics.

Mr. Kaiser has B.S. and M.S. degrees (Mechanical Engineering) from the Swiss Federal Institute of Technology (ETH), in Zurich, Switzerland.

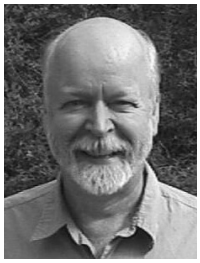

Richard H. Osman is Principal Product Engineer for Siemens Large Drives-Applications (formerly Robicon), in Pittsburgh, Pennsylvania. He serves as technical advisor to the company and works closely with the product development group at Robicon. He has previously worked for: Westinghouse Electric Corporation, developing a variety of solid-state VFDs; Robicon Corporation, as Development Engineer, where he designed special purpose thyristor DC-drives; Manager of AC-Drives Engineering at Robicon; and Technical Director of Heenan Drives Ltd.. He served for five years as Robicon's representative to the NEMA adjustable-speed drives subcommittee and two years as Chairman. He was Director of Drives Engineering at Halmar Robicon Group, Vice-President of Integrated Product Development, and Senior Vice-President of Technology for High Voltage Engineering.

Mr. Osman received a BSEE degree (1965) from the Carnegie Institute of Technology. He has written a number of technical papers on VFDs, is a registered Professional Engineer, and a Senior Member of IEEE.

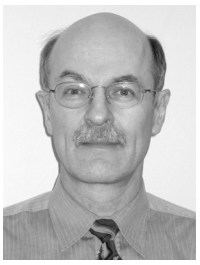

Ralph O. Dickau is a Senior Engineering Specialist with Enbridge Pipelines, in Edmonton, Alberta, Canada. His responsibilities include pumping equipment specifications, selection, installation, and startup. He was team leader for several large pump and motor replacement and rerate programs on the pipeline system. Mr. Dickau is also responsible for troubleshooting pump and motor operating problems. He has presented seminars on pump technology for other pipeline companies through Enbridge Technology, has authored several technical papers, and has been with Enbridge for 24 years.

Mr. Dickau received a B.Sc. degree (Mechanical Engineering, 1978) at the University of Alberta and is a registered Professional Engineer in the Province of Alberta.

ABSTRACT

The use of variable frequency drives (VFD) in pumping applications with variable-duty requirements provides the user with a variety of benefits, including potentially significant energy savings and improved reliability achieved by means of speed reduction and avoiding part-flow operation. Energy savings are primarily realized by running the equipment at high levels of efficiency and optimal operating speeds, matching the generated pump head to the exact system requirements without the use of energy consuming control valves. Running pumps at lower operating speeds and avoiding part-flow operation also positively influences component life and between maintenance intervals. The primary mechanical challenge of any VFD application is the wide continuous operating speed range. Excitation frequencies of fixed speed applications miss most natural frequencies of the structure, rotor, etc., and therefore potentially harmful resonance conditions often do not occur. This is no longer the case with VFD applications, where excitation frequencies become variable and the likelihood of encountering resonance conditions is greatly increased. Problems

and failures in pumps and associated systems that are not caused by resonance are generally not VFD related and are therefore not discussed.

The paper gives an overview of medium-voltage VFD technology as well as the main categories of resonance conditions of concern with regard to mechanical vibrations of pump/motor sets. The analytical and experimental identification of resonances related to lateral rotor, torsional rotor, structural, and acoustic dynamics are discussed in detail. The applicable set of analyses and, if necessary, the corresponding appropriate corrective measures, are designed to help ensure operation free of harmful resonance conditions and problems caused by excessive mechanical vibrations.

INTRODUCTION

Continuous operation under resonance conditions may result in excessive equipment vibrations, reduced in-between maintenance intervals, and premature equipment failure. Resonance conditions with centrifugal pump applications can be divided into the four categories of *lateral rotordynamics, torsional rotordynamics, structural dynamics,* and *acoustic resonance*. Each of these categories requires its own specific set of analyses and checks allowing up-front identification of resonance conditions and corresponding corrective action. Resonances may then be avoided, moved (to operating points where the resulting mechanical vibrations are acceptable), or be detuned altogether. These analyses can also help eliminate the need for expensive factory string tests aimed at investigating vibration performance.

A basic understanding of the most commonly applied and available variable frequency drive (VFD) technology and its rapid development over the last few decades is helpful in the assessment of VFD-related vibration problems and the selection of the optimal set of analyses and checks.

The case studies presented in this paper give a detailed illustration of the analysis procedures and methods that can be employed in order to successfully identify resonance conditions of concern with VFD applications. The same methods and tools can also be used to study the effect of design modifications aimed at detuning resonances. The actual analysis work should be carried out by individuals specifically trained for the task. On a broader level, the paper indicates the type of analyses and checks considered necessary as well as standard analyses that may be omitted. The information presented may therefore be used as an end-user guideline for selecting/purchasing of analysis support from the original equipment manufacturer (OEM) or engineering consultants.

The rotordynamic software tools used for the case studies are pump OEM in-house developments. Commercially available rotordynamic software may be used instead. All structural analyses were performed applying a general purpose finite element analysis software.

EXCITATION SOURCES AND AMPLIFIERS

This section describes the relevant excitation mechanisms and amplifiers of mechanical vibrations.

Mechanical and Hydraulic Unbalance

Mechanical unbalance occurs when the mass centerline of a rotating component does not coincide with the shaft centerline. A certain level of dissymmetry of the weight distribution is unavoidable in rotating equipment. For the case of two-plane balancing, the unbalance measured in US customary units is defined in Equation (1). The factor K is a balance constant, W is the mass per balance plane (or journal), and N is the rotor speed. The SI unit equivalent definition is shown in Equation (2) with the ISO Balance Quality Grade G, rotor-mass m, and the angular speed of rotation ω. The unbalance force rotates with rotor speed (1×) and is therefore a sinusoidal function of time when viewed in a stationary (nonrotating) coordinate system. The corresponding definition of the unbalance force F in US units and SI units is given in Equations (3) and (4), respectively.

$$U = K * \frac{W}{N} \tag{1}$$

$$U = G * 10^{-3} * \frac{m}{\omega / 60} = G * 10^{-3} * \frac{m}{2\pi * N / 60} \tag{2}$$

$$F = U * 0.000162 * \omega^2 \sin(\omega t + \varphi) \tag{3}$$

$$F = U\omega^2 \sin(\omega t + \varphi) \tag{4}$$

Geometric deviations between the individual impeller channels create a nonuniform pressure distribution at the impeller outlet, which also rotates with rotor speed (1×). The resulting radial hydraulic force has much the same effect as mechanical unbalance and is therefore referred to as hydraulic unbalance. Hydraulic unbalance increases with increasing flow-rate and usually exceeds mechanical unbalance by factors. Unbalance affects lateral rotor and structural vibrations but not torsional rotor vibrations.

Self-Excited Vibration

Self-excited vibration, also known as rotor instability, is most commonly associated with radial journal bearings, annular seals, and hydraulic impeller-casing interaction. Self-excited vibration caused by lightly loaded cylindrical journal bearings/guide bearings in vertical pump application are the most common cause of instability in centrifugal pumps. The corresponding vibration frequency typically lies between 0.40 and 0.50 times running speed (subsynchronous vibration), indicating a tangential mean fluid velocity c_u inside the tight bearing clearance per Equation (5). The parameter R denotes the rotor radius at bearing location and ω is the angular shaft speed.

$$c_u = 0.40...0.50 * \omega * R \tag{5}$$

Pumps with excessively worn annular seals can show the same phenomenon with vibration frequencies in the 0.7 to 0.9 times running speed range (also above 1× running speed in case of tangential fluid entry velocities > ωR).

Instabilities are caused by the nonsymmetrical pressure distribution of the vibrating shaft, which creates a force component acting in the direction of the shaft orbit. This force feeds energy to the rotor and thus the shaft orbital movement is accelerated. Instability occurs in case the energy put into the rotor exceeds the direct damping opposing the same vibration.

Many vertical pump applications show a vibration component at or near 0.5× running speed in their amplitude spectrum (also referred to as oil whirl or bearing whirl). Instability usually only occurs in case a structural or lateral rotor natural frequency is at or near this 0.5× running speed frequency, changing the oil whirl into an oil whip condition with potentially destructive vibration levels. In case the operating speed is increased after the onset of instability, the vibration frequency will typically remain nearly constant, locked into the natural frequency of the structure or rotor as indicated in Figure 1.

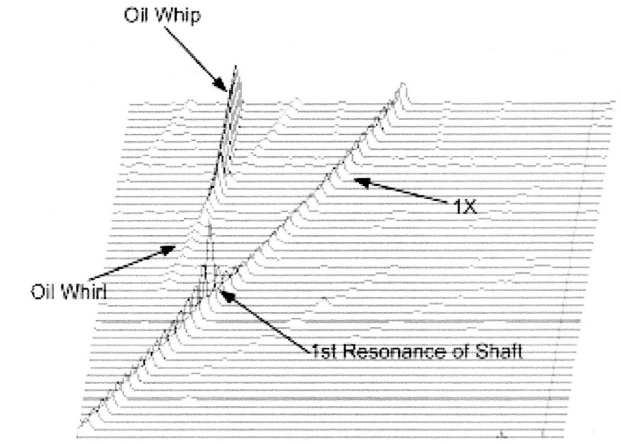

Figure 1. Waterfall Vibration Plot.

Measures against self-excited vibration include:

- Reducing the mean tangential velocities in journal bearing and annular seal tight clearances. This may be achieved by means of applying rough stator surface finish, swirl breaks at annular seal entry, stator-side honeycomb or hole patterns, smooth rotor surface finish, etc.
- Increasing bearing radial load by means of applying additional (intentional) misalignment in vertical pumps.
- Avoiding critical speed situations between 0.5× running speed excitation and lateral or structural natural frequencies.
- Restoring design clearances in case of excessively worn annular seals.

Self-excited vibrations affect lateral rotordynamics and structural vibrations, not torsional rotordynamics.

Vane-Pass Pressure Pulsations

Vane-pass pressure pulsations are generated by the impingement of the nonuniform impeller wake flow on the volute cutwater or diffuser vane tips. Figure 2 depicts the nonuniform fluid velocity profile at the impeller outlet. These pressure pulsations travel through the system at the speed of sound of the pumpage. The frequency of the vane-pass pressure pulsations, acting on the stator, is proportional to the pump rotational speed N, the impeller vane count z_2, and multiples (n) thereof as illustrated in Equation (6).

$$f_{VANE-PASS} = n * z_2 * (N / 60) \quad \textbf{(6)}$$

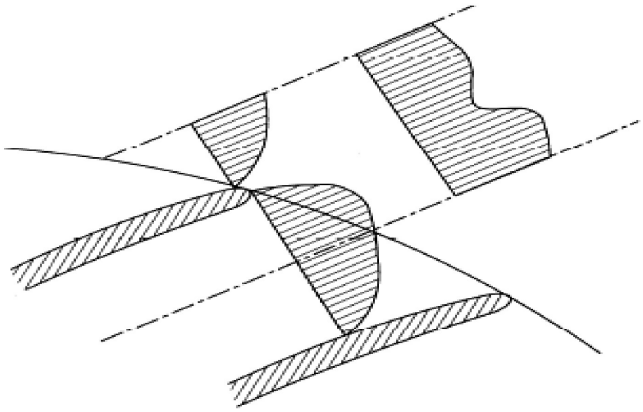

Figure 2. Wake Flow at Impeller Outlet.

The main factors influencing the pressure pulsation magnitude are the radial gap between the impeller outer diameter and the volute/diffuser cutwater (B-gap), the percent of best efficient point (BEP) operation, and the impeller outlet velocity u_2.

B-Gap

The radial distance between the impeller vane trailing edge and the volute cutwater or diffuser vane leading edge (B-gap) heavily influences the pressure pulsation amplitudes. According to investigations published in (Guelich and Bolleter, 1992), pressure pulsation amplitudes decrease on average with a power of (−0.77) on the relative radial gap as illustrated in Equation (7). For example, a 2 percent B-gap will produce pressure pulsation amplitudes three times higher than a 9 percent B-gap on an otherwise identical pump.

$$\Delta P* \approx \left(\frac{D_3}{D_2} - 1 \right)^{-0.77} \quad \textbf{(7)}$$

Percent BEP Operation

In Figure 3, statistical data from 36 measurements of single and multistage pumps are plotted as dimensionless root mean squared (rms) values for the frequency range of 1.25 to 20 times running speed, which covers vane-pass frequency. Pressure pulsations are normalized according to Equations (8) and (9) for US units and SI units, respectively. ΔP_{RMS} is the rms value of the dimensional pressure pulsation measurement, ρ is the fluid density, and u_2 is the fluid velocity at impeller outlet. Flow is normalized as shown in Equation (10) with Q being the effective flow and Q_{BEP} representing the best-efficiency flow. The curves displayed in Figure 3 shows the strong dependency of pressure pulsations from the operating point with reference to percent of BEP operation (Guelich and Egger, 1992).

$$\Delta P*_{RMS} = \frac{9269 * \Delta P_{RMS}}{\rho * u_2^2} \quad \textbf{(8)}$$

$$\Delta P*_{RMS} = \frac{2 * \Delta P_{RMS}}{\rho * u_2^2} \quad \textbf{(9)}$$

$$q* = Q / Q_{BEP} \quad \textbf{(10)}$$

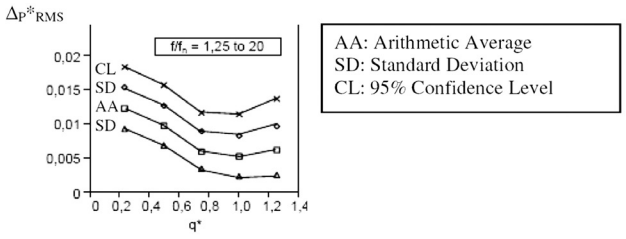

Figure 3. Pressure Pulsations Versus Percent of BEP Operation.

Impeller Outlet Velocity

Experience indicates that pressure pulsations in geometrically similar pumps roughly increase with the square of the circumferential speed as shown in Equations (11) and (12) for US units and SI units, respectively:

$$\Delta P_d = 0.75 * 0.000162 * \frac{\rho}{2} u_2^2 \quad \textbf{(11)}$$

$$\Delta P_d = 0.75 * \frac{\rho}{2} u_2^2 \quad \textbf{(12)}$$

The stagnation pressure ΔP_d is a measure of the unsteady hydrodynamic load acting on the volute or diffuser vane.

Other Influencing Parameters

Parameters affecting the nonuniformity of the impeller wake flow and geometric parameters have an influence on the generation and amplitude of pressure pulsations. Among these parameters are:

- Thickness and form of the impeller vane trailing edge.
- Number of impeller vanes and combination of impeller vanes to volute vanes/diffuser vanes (e.g., odd versus even number of impeller vanes in double volute type pumps).
- Impeller specific speed. Pressure pulsations generally increase with increasing specific speed.
- Impeller geometry, particularly vane exit angle and shape of volute cutwater (blunt versus hydraulically smooth).
- Staggering of impellers along shaft of multistage pumps and staggering of the two halves of double suction impellers.

Vane pass pressure pulsations primarily affect structural vibrations (e.g., bearing housing vibrations). A certain pressure pulsation level will always be present in centrifugal pumps and does not need to represent a problem. Excessive pressure pulsations can result in high pump and piping vibrations, particularly in combination with structural resonance or acoustic resonance. This may result in vibration levels beyond alarm or shutdown and cause fatigue failures in auxiliary piping, instrumentation, etc.

Other Excitation Sources

Other excitation sources include broadband hydraulic forces due to recirculation, cavitation, and forces due to rotating stall.

Amplifiers

Vibration levels usually become excessive when amplified by resonance. A resonance condition occurs when an excitation frequency is within a few percent of a relevant natural frequency. In that condition, the excitation force is acting again once the vibrating component has come full cycle after the last "impact" by the force. The excitation force and the vibration are synchronized, and the vibration amplitude increases until limited by nonlinear effects. With regard to mechanical vibrations in VFD operated centrifugal pumps, resonance conditions can be divided into four categories: structural resonance and torsional rotor resonance are typically lowly damped and are likely to result in high levels of mechanical vibration when properly excited. Lateral rotor resonances are in some cases highly damped and operation on or near such a condition ("critical speed") may be perfectly acceptable. Acoustic resonance conditions, amplifying mechanical vibrations via amplified pressure pulsations, are usually only lowly damped. The various resonance categories are discussed in detail in the following sections.

LATERAL ROTORDYNAMICS

General

The damped lateral rotordynamic behavior of a centrifugal pump rotor is determined by the rotor geometry, the rotor mass and inertia, and the interaction forces occurring between the rotor and journal bearings, annular seals, and casing. Impeller wear rings, close-clearance bushings, and balance pistons are typical examples of annular seals. Casing interaction occurs at impeller location, between the wear rings in case of a closed impeller design, and is generally destabilizing. These interaction forces are nonlinear but may be linearized around a particular static rotor equilibrium position. Interaction forces vary with operating speed, pumpage specific gravity and viscosity, load, state of wear, etc. Solving the linearized homogeneous Equation of Motion (13) results in a set of eigenvalues.

$$\underline{\underline{K}}\,\underline{x} + \underline{\underline{D}}\,\underline{\dot{x}} + \underline{\underline{M}}\,\underline{\ddot{x}} = \underline{0} \tag{13}$$

The linearized equation of motion consists of a stiffness-matrix K, damping-matrix D, mass-matrix M, and vectors of displacements (x), velocity ($\dot{x}$), and acceleration ($\ddot{x}$). The complex eigenvalue λ_X is defined in Equation (14). The imaginary component ω_X represents the angular natural frequency. The eigenvalue determines the corresponding natural frequency f (Equation [15]), modal damping value D (Equation [16]), and mode shape as shown in Figure 4. A mode with negative damping D represents an instable system. The rotor system is laterally stable when all significant modes provide positive modal damping levels.

$$\lambda_x = \alpha_x + i*\omega_x \tag{14}$$

$$f = 2*\pi*\omega_x \tag{15}$$

$$D = -\frac{\alpha_x}{\sqrt{\alpha_x^2 + \omega_x^2}} \tag{16}$$

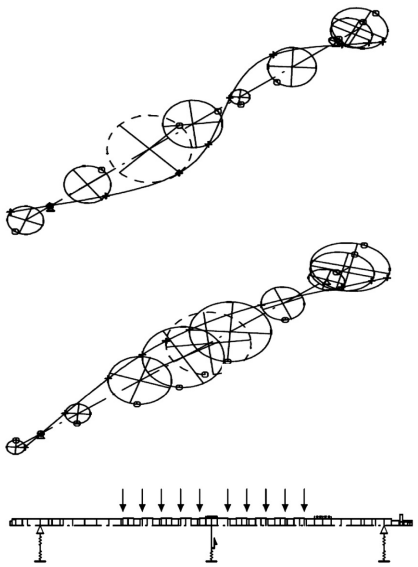

Figure 4. Lateral Mode Shapes and Mechanical Model.

The evaluation of the lateral rotordynamic behavior can either be done by solving the homogeneous equation of motion (eigenvalue calculation) or by specifying a set of excitation forces and subsequent solution of the nonhomogeneous equation of motion (forced response analysis).

The eigenvalue approach and evaluation of results applying a combined frequency-versus-damping-ratio criterion is further discussed in this paper. This approach is less ambiguous compared to a forced response analysis because it avoids the subjective process of determining and applying excitation forces (typically a combination of mechanical and hydraulic unbalance loads).

The results of a damped lateral rotordynamic analysis are best presented in the form of a Campbell diagram as illustrated in Figure 5, plotting the natural frequencies and modal damping factors versus pump operating speed. The intersection between a speed-dependent natural frequency line and the synchronous speed excitation line is called a critical speed and represents a resonance condition.

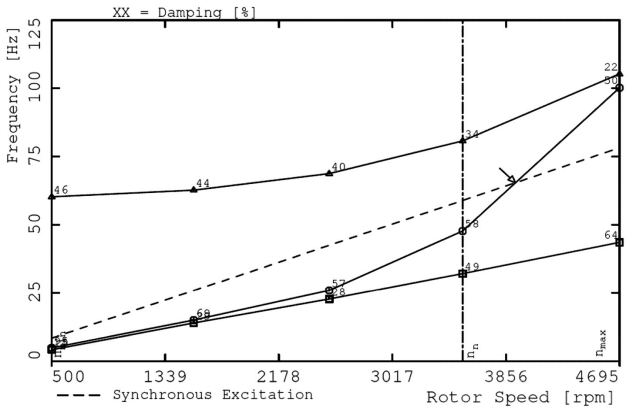

Figure 5. Campbell Diagram.

A widely used eigenvalue acceptance criterion is defined in Annex I of the API 610 standard (Eighth Edition, 1995; Ninth Edition, 2003; Tenth Edition, 2004) and the ISO 13709 standard (2003), respectively. The combined frequency-versus-damping criterion, depicted in Figure 6, is applied to each of the calculated lateral modes, limiting the evaluation to modes within a natural frequency range of zero to 2.2 times running speed. This frequency range covers the most typical and significant rotor lateral excitation forces including subsynchronous excitation, mechanical and hydraulic unbalance and misalignment:

- Subsynchronous excitation (journal bearings): 0.4… 0.5× running speed (typical)
- Subsynchronous excitation (annular seals): 0.7… 0.9× running speed (typical)
- Rubbing: multiples of 0.5×
- Mechanical unbalance: 1× running speed
- Hydraulic unbalance: 1× running speed
- Misalignment: 1× and 2× running speed

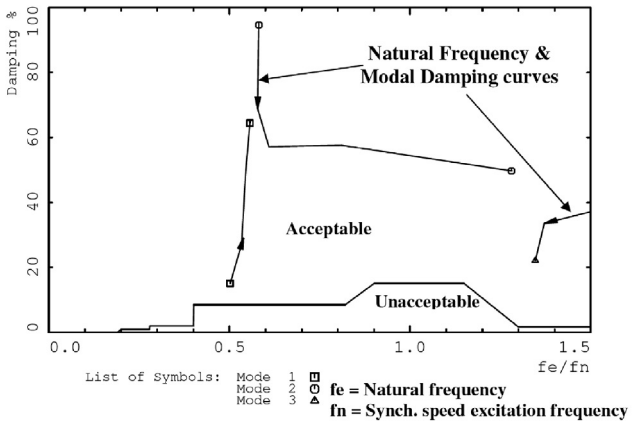

Figure 6. API 610 Lateral Rotordynamic Acceptance Criterion.

The API 610 (2004) lateral evaluation criterion also requires consideration of operating speeds outside of the defined pump continuous operating speed range. A speed range of 25 percent of minimum continuous speed to 125 percent of maximum continuous operating speed needs to be investigated.

While, for cases in violation, the cited API standards allow proof of acceptability by means performing additional unbalance forced response analysis, this approach is not recommended for obvious reasons. An unbalance forced response analysis applies excitation sources at synchronous speed (1×), which cannot excite subsynchronous modes. It is therefore recommended to consider the modal-damping-versus-frequency-separation acceptance criterion illustrated in Figure 6 as binding. With a few exceptions not discussed in this paper, rotor designs in violation should be modified to meet this acceptance criterion. Design modifications aimed at improving lateral rotordynamic stability can be divided in two categories. A first category aims at increasing the frequency separation margin between lateral modes and synchronous excitation speed by means of increasing the rotor stiffness (K_{xx}) or reducing the rotor mass (M). A second category of modifications intends to increase modal damping.

Design modifications aimed at increasing lateral rotor natural frequencies:

- Decreasing coupling overhung length and/or coupling weight in case of overhung dominated modes (K_{xx}, M)
- Changing of impeller material from steel to aluminum (M)
- Increasing shaft size (K_{xx})
- Decreasing between-bearing span (K_{xx})
- Tightening or restoring annular seal clearances (K_{xx})
- Eliminating stator-side serrations applied to reduce leakage (K_{xx})
- Applying stator-side circumferential grooves in balance pistons and center and throttle bushings. This reduces the adverse effect of piston tilting onto the direct radial annular seal stiffness (K_{xx}).
- Changing from inline to back-to-back configuration, which reduces bearing spans and also adds damping at the center of the pump (K_{xx})

Design modifications aimed at increasing modal damping:

- Applying stator-side swirl breaks at the entrance of impeller eye wear rings. This reduces the circumferential inlet swirl, which in turn reduces destabilizing annular seal cross-coupled stiffness.
- Optimizing the journal bearing design. Journal bearings with length-over-diameter ratios above one should be avoided. The destabilizing effect of cross-coupled journal bearing stiffness can be reduced or eliminated by switching from cylindrical bearings to multilobe or tilting-pad designs.
- Loading of vertical pump line-shaft bearings by means of applying intentional misalignment between bearings and rotor
- Applying rough annular seal stator surface finish, stator-side honeycomb or hole patterns, smooth rotor surface finish

In case a fixed speed centrifugal pump is converted to VFD operation, the *continuous VFD operating-speed range may already be sufficiently analyzed and covered by the original fixed-speed lateral rotordynamic analysis*. Fixed-speed lateral analyses should be carefully reviewed on a case-by-case basis before deciding whether a new lateral analysis for the VFD operated application is necessary or not.

Case Study—Standard Lateral Rotordynamic Analysis Procedure

The dynamic lateral stiffness and damping levels provided by the journal bearing fluid film depend on the stiffness of the bearing housing/support structure itself. With most horizontal pumps, the lowest bearing housing natural frequency is well above the first few lateral rotor bending mode natural frequencies. In these cases, the corresponding *journal bearing support stiffness can be considered as near-rigid and constant over the entire speed range* of concern. The situation is entirely different with most vertical pump applications. Vertical pumps are typically structurally flexible and significant structural modes may appear at, near, or below operating speed. This requires calculation of the dynamic bearing support stiffness by means of performing harmonic response

analyses of the entire pump and motor structure. Alternatively a rotordynamic code capable of performing a combined rotor-structure analysis may be employed.

The process of vertical pump lateral rotordynamic analysis is explained using the example of a water transport booster pump. The vertical turbine is VFD operated with a continuous operating speed range of 257 to 514 rpm and driven by a 900 horsepower asynchronous electric motor. The pump featuring a 42 inch diameter discharge nozzle and 48 inch diameter columns generates 45 feet of differential head, moving 55,555 gpm while running at 514 rpm rated speed.

The forced harmonic response analyses were performed applying a general purpose finite element software program using beam elements for modeling of motor and pump structure. The inertia and mass effects of the rotating element were considered applying lumped mass elements attached to the structure at bearing holder and impeller locations. Internal and surrounding water effects were considered as additional mass effects applied to the beam elements. The stiffness effect of the receiver-can flange and gusseting was determined in separate static finite element (FE) analyses and considered via spring elements in the forced harmonic response model. Figure 7 depicts the calculated static receiver-can deflection due to unit-moment loading in the horizontal direction.

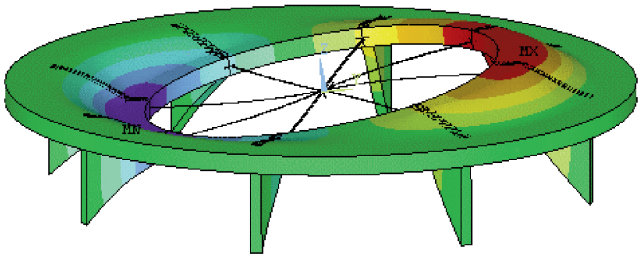

Figure 7. Calculated Receiver Can Flange Deflection.

Figure 8 shows the first three structural modes of the pump and motor structure as a result of a modal structural FE analysis. The modes occur at 2.6 Hz (156 cpm, first column mode), 14.2 Hz (852 cpm, first aboveground mode), and 20.5 Hz (1230 cpm, second column mode), respectively. The dynamic bearing support stiffnesses required for the lateral rotordynamic analysis are calculated in a series of forced harmonic response analyses. Each of these analyses applied a dynamic unit-load at a single bearing location and varied the frequency of this harmonic load within a specified frequency-range. Figure 9 illustrates the dynamic displacement response at the upper motor bearing due to harmonic excitation (unit force in lateral direction acting at the same location). The response indicates an amplitude response peak at approximately 15 Hz, which corresponds to the second structural mode showing large modal displacement in the aboveground portion of the machine.

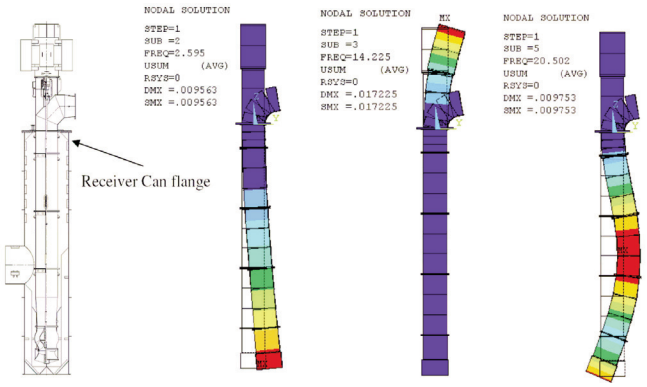

Figure 8. First Three Pump Structural Mode Shapes.

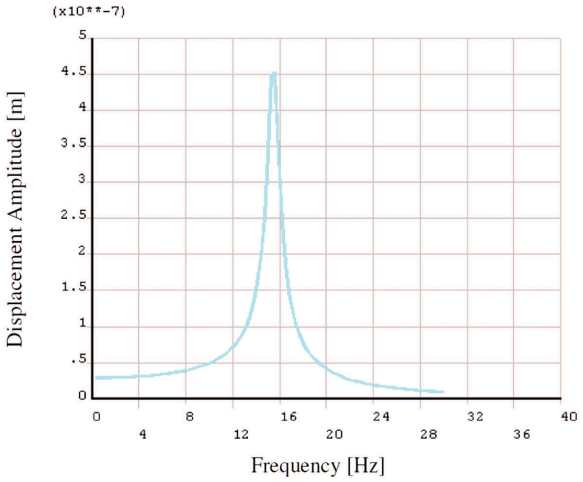

Figure 9. Amplitude Response at Upper Motor Bearing.

Figure 10 shows a Bode plot of the dynamic response at the suction-bell bearing due to harmonic excitation at the same location. Amplitude responses at approximately 2.5 Hz and 20.5 Hz correspond to the first and third structural mode natural frequencies.

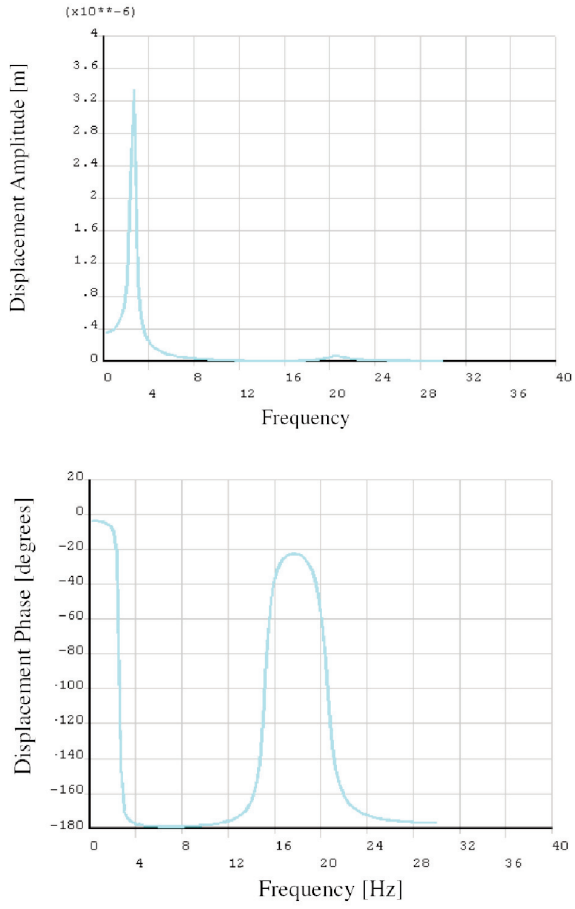

Figure 10. Bode Plot of Response at Suction-Bell.

The calculated displacement curves $U_{XX}(f)$ are inverted to derive the various dynamic stiffness curves $K_{XX}(f)$ as indicated in Equation (17) and displayed in Figure 11.

$$K_{xx}(f) = 1 / U_{xx}(f) \qquad \textbf{(17)}$$

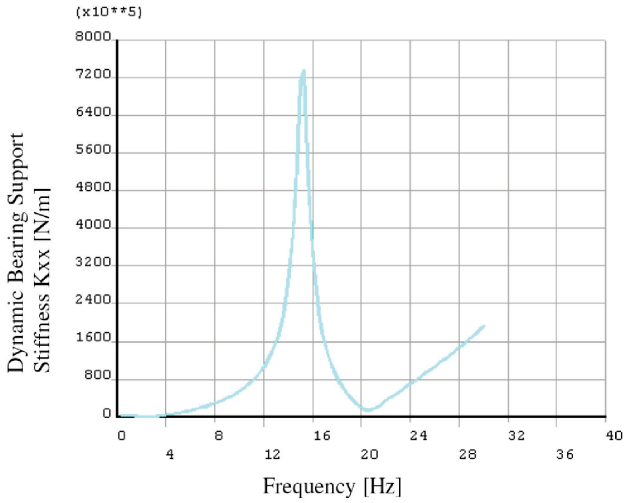

Figure 11. Dynamic Bearing Support Stiffness $K_{XX}(f)$ at Suction Bell.

The subsequent lateral rotordynamic analysis applied unbalance loads based on an ISO 1940-1 Grade G2.5 (equivalent to an API balance grade of 15 W/N; IRD Balancing, 2007), evaluated at rated operating speed. The corresponding unbalance forces in the lateral forced response analysis are varied proportional to the square of the operating speed. The significant shaft response peaks lay outside of the continuous VFD operating speed range and are therefore not an operational concern. However, the analysis clearly proves that *shaft amplitude response peaks can occur at the natural frequencies of the structure* (refer to Figures 12 and 13 for details).

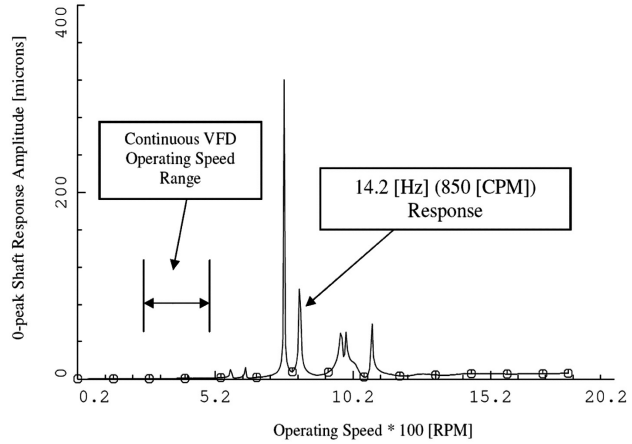

Figure 12. Lateral Shaft Response Amplitude at Upper Bearing.

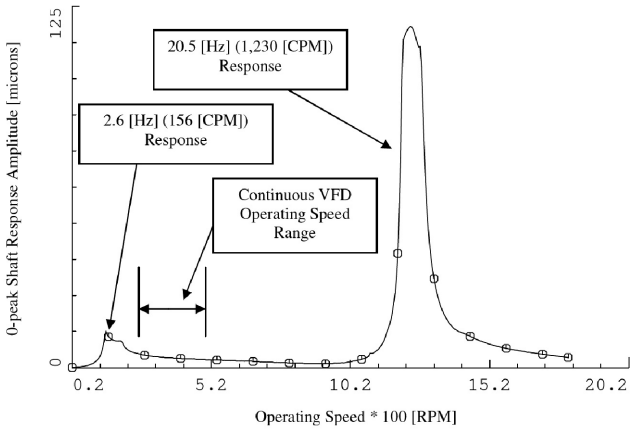

Figure 13. Lateral Shaft Response Amplitude at Suction Bell.

Case Study—Rotor Instability

Vertical pump bearings and bushings are typically only lightly loaded, which may cause rotor instability problems. The phenomenon is explained on the example of a vertical mixer pump intended for VFD operation in slurry mixing service. The single-stage, quad-volute pump, driven by a 200 horsepower asynchronous motor, underwent an endurance test at the OEM factory. The pump design features seven columns of 16 inch diameter, supporting the 2 inch diameter shaft at seven line-shaft bearing locations. The bearing material is nickel-impregnated carbon mounted in bearing holders that were initially loosely positioned between column flanges. At startup, shaft vibration readings taken at the bottom seal location showed two distinct peaks of both approximately 1.2 mils peak-to-peak at 1× and 0.5× running speed frequency. The 50 percent running speed frequency represents "bearing whirl." The bearing whirl frequency decreased almost linearly over time starting from 18.5 Hz, indicating wearing out carbon bushings. A post-test inspection revealed that the diametrical bushing clearances increased from an initial 7 mils design clearance to as much as 400 mils. The failed test triggered analyses and modal testing. Lowly damped lateral rotor modes at approximately 50 percent running speed and structural column modes at 0.2, 4.5, 14.0, and 29.0 Hz were calculated and support-structure modes at 10 and 26 Hz were measured by means of modal testing. Figure 14 illustrates the frequency and amplitude of column vibrations filtered to synchronous speed and bearing whirl frequency, respectively. The bearing whirl frequency decreases linearly with time, obviously because of continuous wear of the carbon bushings. After approximately 35 hours, the bearing whirl frequency started to lock into the third column natural frequency for a few hours (bearing whip condition), resulting in amplified vibration levels.

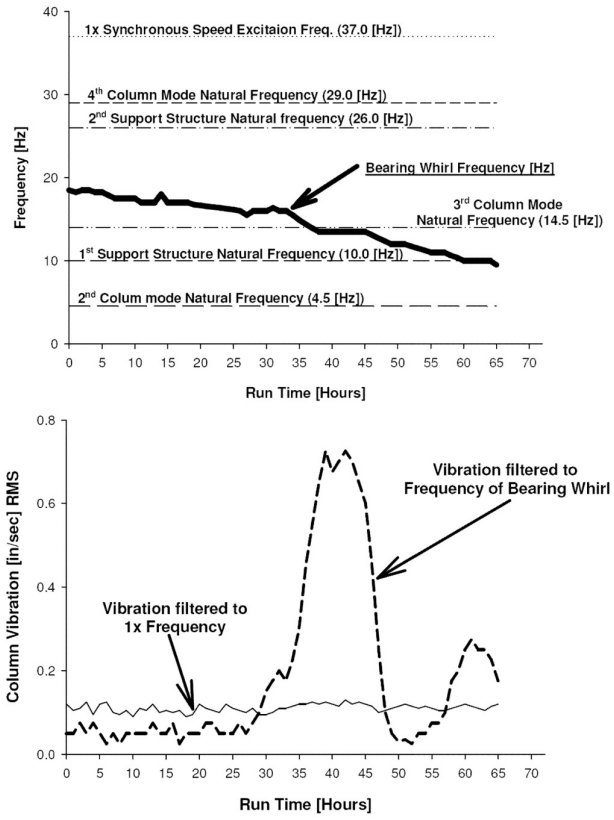

Figure 14: Column Vibration and Natural Frequencies.

The pump was successfully retested after implementation of design changes, which included fixation of the initially loose bearing holders, built-in misalignment between the bearing holders

and the shaft, as well as structural modification of the pump support structure. The successful retest did not show any significant bushing wear and the bearing whirl frequency remained constant throughout the test.

Conclusions

Horizontal Pumps

When converting a fixed speed application to VFD operation, the original lateral rotordynamic analysis may already sufficiently cover the new application. However, a careful review of the results of the original analysis and the new operating conditions is required on a case-by-case basis. The speed range above the original fixed operating speed requires special attention because of the increased power absorption and the increased likelihood of encountering critical speeds, for example critical speeds with coupling overhung dominated modes. The primary excitation mechanism of concern is synchronous speed excitation due to mechanical and hydraulic unbalance. API 610 Eighth through Tenth Editions (1995, 2003, 2004), Annex I, defines a reasonable lateral rotordynamic acceptance criterion.

Vertical Pumps

A significant coupling between the dynamic behavior of the structure and lateral rotordynamics is often the case. The frequency of lateral modes can coincide with structural natural frequencies, resulting in amplified shaft vibrations. The correct assessment of a vertical pump lateral rotordynamic behavior requires a combined lateral-structural analysis covering the entire continuous VFD operating speed range. Significant structural natural frequencies at 1× and 0.5× running speed should be avoided. The primary excitation mechanisms of concern are synchronous speed excitation (unbalance) and subsynchronous speed excitation around 50 percent of running speed (bearing whirl).

In case a resonance condition cannot be detuned, it is also possible to lock out/program out a specific operating speed range from continuous operation.

TORSIONAL ROTORDYNAMICS

General

Torsional vibration problems usually involve resonance conditions. Torsional resonance occurs when a train torsional natural frequency coincides with or is close to an applicable excitation frequency. Due to the substantial torsional stiffness of both rigid and flexible disc type couplings, the entire shaft train needs to be analyzed.

Shaft trains driven by electric motors are subject to transient and steady-state excitation. There are two transient excitation sources of concern, which are startup and short-circuit fault condition. Startup occurs at line frequency and short circuit excitation functions include one- and two-times line frequency components.

Potential steady-state excitation sources are:

- The 2× running speed excitation represents an interaction between lateral and torsional vibration. In case of an elliptical, i.e., noncircular, shaft orbit (1× lateral shaft vibration), the forces necessary to keep the shaft on its orbit result in an alternating moment acting on the shaft. This moment changes its amplitude twice per revolution, and therefore represents a dynamic torsional excitation source acting at 2× running speed frequency.
- Vane-pass frequency excitation is another potential mechanism but it was found to be significant only in case of impellers with a low number of vanes and relatively thick vanes as applied in sewage pumps.
- VFD operated pump trains are subject to VFD torque harmonics, often occurring at multiples of 6× feed-frequency.
- Some literature mentions 1× running speed as a torsional excitation frequency. However, shaft trains without gearboxes usually exhibit only negligible 1× torque harmonics.
- Shaft trains with a gearbox have additional steady-state torsional excitation sources that occur at 1× running speed (pitch cycle runout), gear-mesh frequency (based on the number of gear teeth), and pinion-mesh frequency (based on the number of pinion teeth).

The applicability of the above described excitation sources with regard to VFD operated shaft trains is further discussed.

Similar to the recommended procedure for lateral rotordynamic analyses, the torsional rotordynamic behavior of a shaft train is best analyzed by means of a natural frequency analysis, subsequent evaluation of resonance conditions, and, if necessary, performing of transient and/or steady-state forced response analyses. The standard torsional natural frequency analysis is an undamped analysis. An undamped natural frequency analysis applies because virtually all shaft trains only provide low levels of torsional damping. The damped and the corresponding undamped natural frequency do not significantly differ in case of low modal damping. Equation (18) explains the relationship between the damped and undamped natural frequency of a single degree of freedom system. In the example of a 50.0 Hz undamped natural frequency and a 3 percent critical damping ratio, the damped natural frequency drops to only 49.98 Hz.

$$f_{DAMPED} = f_{UNDAMPED}\sqrt{1-D^2} \quad \textbf{(18)}$$

The results of a torsional natural frequency analysis are again best presented in the form of a Campbell diagram, plotting the speed-independent natural frequency lines together with potential excitation frequencies. Forced response analyses apply forcing functions at their corresponding load-induction locations. Startup and short circuit excitation, for example, induce their load at the motor core. The outcome of a forced response analysis may be a plot of torsional stress along the entire shaft at a set constant operating speed. The forced response analysis can also be used to calculate the torsional stress at a specific shaft location of interest, varying the operating speed (frequency-sweep). In any case, the stress results can be further used in fatigue analyses in order to evaluate the acceptability of the investigated resonance condition(s).

Case Study—Standard Torsional Rotordynamic Analysis Procedure

The torsional rotordynamic analysis procedure is demonstrated on the example of an axially-split, horizontal, multistage barrel-type pump in crude oil transfer service. The 10×10×13.5 CP 10 stage pump is VFD operated with a continuous operating speed range of 2000 to 3755 rpm. Figure 15 shows an isometric view of the pump assembly.

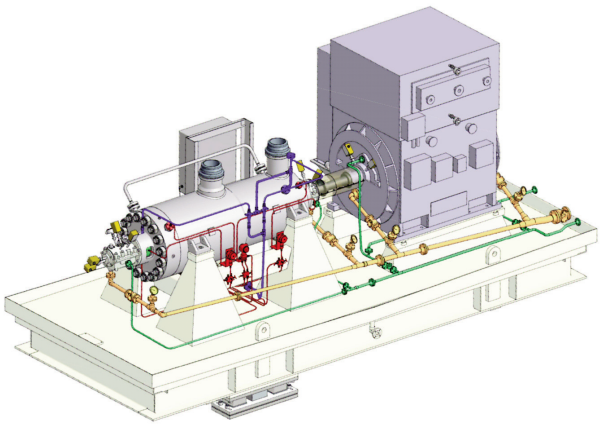

Figure 15. Isometric View of Pump Assembly.

The results of the natural frequency analysis are presented in the Campbell diagram displayed in Figure 16. Mode shapes and the mechanical model are shown in Figure 17. The Campbell diagram includes 2× running speed excitation and the first three VFD torque harmonic excitations at 6×, 12×, and 18× running speed.

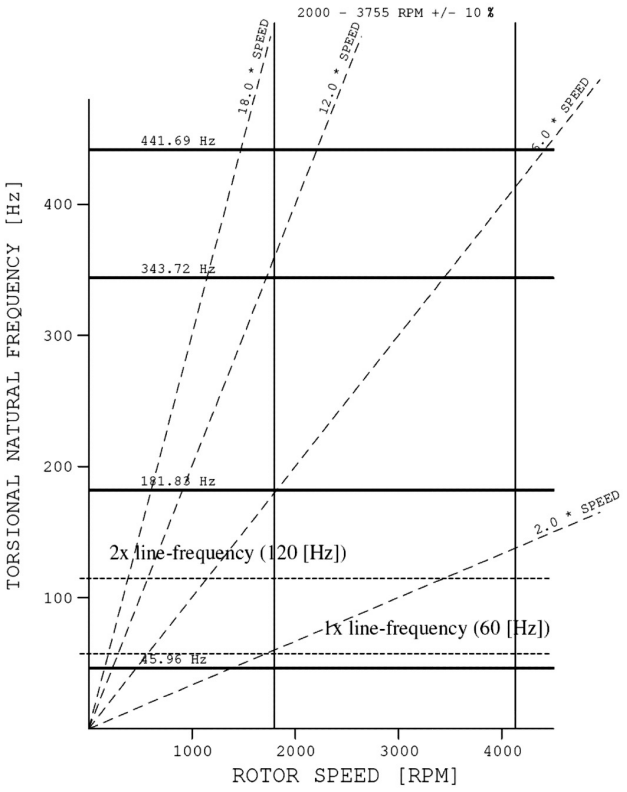

Figure 16. Torsional Campbell Diagram.

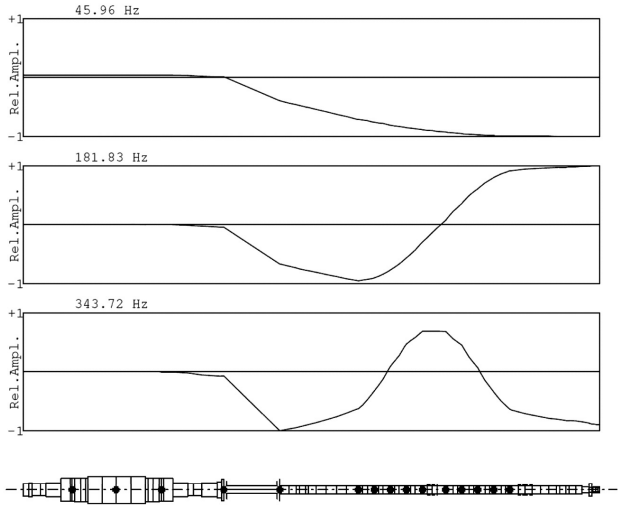

Figure 17. Torsional Mode Shapes.

The natural frequency analysis revealed multiple critical speed situations between torsional modes and steady-state VFD torque harmonics. These resonance conditions have been further investigated in damped forced response analyses applying torque excitation functions provided by the VFD manufacturer. The applied dynamic torque was 2.0 percent (sixth harmonic), 1.5 percent (12th), 2.8 percent (18th) and 1.4 percent (24th) of static torque. Figure 18 plots the calculated torsional stress due to 6× VFD torque harmonic excitation at 1818 rpm operating speed, exciting the 181.8 Hz second torsional mode. The calculated maximum torsional stress is approximately 4.5 psi (0.03 MPa). Stress responses as low as these are normal for torque harmonic excitation from modern, state-of-the-art VFDs.

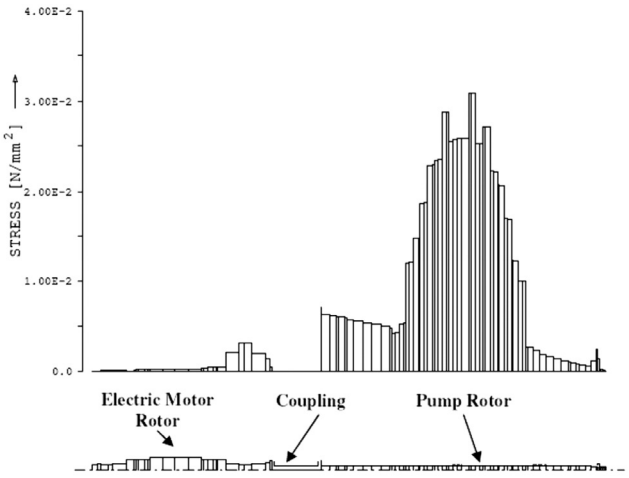

Figure 18. Torsional Stress Response.

Steady-State VFD Torque Harmonic Excitation

Resonance conditions between VFD torque harmonics and torsional modes are often unavoidable because of the large VFD operating speed range. It is technically not feasible to detune these types of critical speeds. The complete review of 43 torsional analyses of VFD operated single and multistage horizontal centrifugal pumps indicated a maximum pump shaft stress due to resonance with VFD torque harmonics of 254 psi (1.75 MPa). The average shaft stress response was 79 psi (0.54 MPa). The above-mentioned stresses do not consider any stress concentration factors, which would be a factor of approximately four at the most.

Once started and running in equilibrium on the utility, polyphase motors produce very little torque ripple (torque harmonics) at the shaft. This assumes that the utility has negligible distortion and unbalance, which is not always the case. Torque ripple increases when a motor is VFD operated. When a perfect/ideal polyphase motor is excited by polyphase sinusoidal currents, the angular velocity of the stator magneto-motive force (MMF) will be perfectly constant. The flux is also sinusoidally distributed around the gap, and thus the angle between flux and MMF remains constant and the torque is therefore a constant also. There are two sources of torque ripple, which are nonsinusoidal currents from the VFD, and motor winding effects. The motor windings are discrete coils in discrete slots, so it is not possible to get a perfectly distributed winding capable of producing a perfectly sinusoidal airgap flux distributed around the gap. Generally these effects are small, leading to motor-created torque ripple in the low single percent range of rated torque. Some motor manufacturers even deny that the motor can produce torque ripple by itself when excited by pure sinusoidal current.

Any practical VFD powerful enough to run a pump cannot operate as a linear amplifier, but must resort to simple “on” or “off” states of the power electronic’s switches. Because of this, there will always be harmonics present in the output voltage and current of the VFD, which is applied to the motor. Due to the three-pole output structure, the harmonics are all odd, with those divisible by three being absent (a pole is the power electronic’s block that creates the output to one phase of the motor). The lower order harmonics (five, seven, 11, and 13) of the fundamental output frequency cause the stator MMF angular velocity to fluctuate slightly. That causes the angle between flux and MMF to vary with a characteristic pulsation frequency. The fifth and seventh current harmonics cause a torque ripple six-times the output frequency, and 11th and 13th harmonics cause 12th order

harmonic torque ripple and so on. Of course the amplitude of the torque ripple is proportional to the amplitude of the current harmonics. The poorest performing VFD in this respect is the load commutated inverter (LCI). This VFD creates a smooth direct current (DC) link current and switches it into the stator windings in a prescribed sequence. The quasi-square wave current causes the stator MMF to advance in steps of 60 degrees electrical at each commutation (a commutation is the transfer of current from one power switch to the next one in sequence). An LCI with two parallel circuits operating into a dual winding motor (12-pulse output) creates 3 to 8 percent torque ripple. Another popular circuit, the neutral point clamped (NPC) circuit has five voltage levels from line-to-line and uses pulse-width modulation (PWM) techniques. Depending on the frequency of switching, the current is less distorted and the torque ripple decreases into the vicinity of 1 percent to 3 percent. A third architecture, the multilevel series-cell circuits, can further reduce the current distortion such that the torque ripple decreases to 1 percent of motor base rating. Multilevel series-cell circuits also apply PWM technology. Figure 19 displays voltage waveforms produced by LCI, NPC, and multilevel series-cell (PWM) VFD architectures. *For the LCI drive system, it is usual practice to perform a torsional rotordynamic analysis of the drive train, investigating critical speeds with LCI-VFD torque harmonics*.

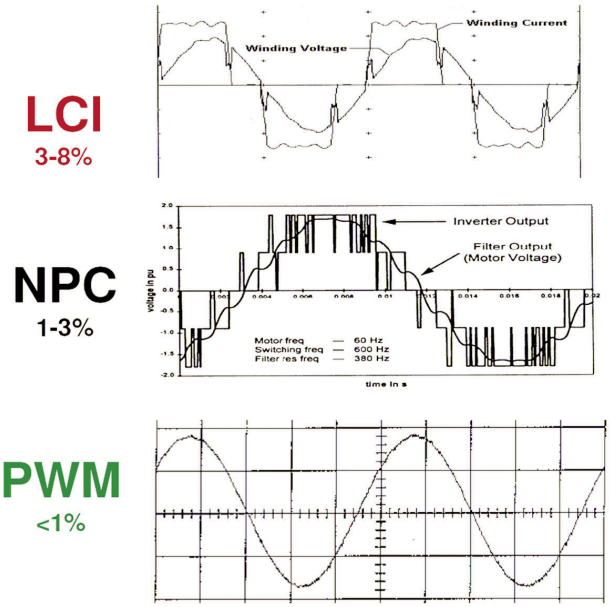

Figure 19. Voltage Waveforms Generated by Different VFD Architectures.

The main technique to reduce torque ripple is to decrease the harmonic content of the output current. That is generally done by increasing the PWM switching frequency, or adding additional voltage levels to the output voltage, or both. For the cases where this is not possible, application of filters is an alternative option. It is common practice to equip VFDs with an L-C (inductor-capacitor) filter on the output to attenuate some harmonic currents in order to reduce motor torque ripples. This technique is used for LCI and NPC VFDs. The disadvantage is that the filter causes extra expense, increased size, and poorer efficiency. For drive systems with high sensitivity to torque ripple, the multilevel series cell designs offer an advantage.

One-Times Running Speed and Vane-Pass Frequency Excitation

Dynamic torque measurements taken at the coupling spacer of the previously described barrel-type transfer pump are presented in Figure 20. The dynamic torque amplitude data are shown as percentages of the corresponding static torque. The readings indicate that the 1×, 2×, and 7× (vane-pass) dynamic torque values are mostly less than 1 percent of static torque. In case of a 1 percent, one-times dynamic torque applied at the first torsional natural frequency, the calculated shaft stress at pump coupling hub location is only 116 psi (0.8 MPa). Conservatively only 1 percent of modal damping was applied in this steady-state forced response analysis. The same dynamic torque measurements did not indicate any significant peaks at 6× VFD torque harmonic frequency and multiples thereof.

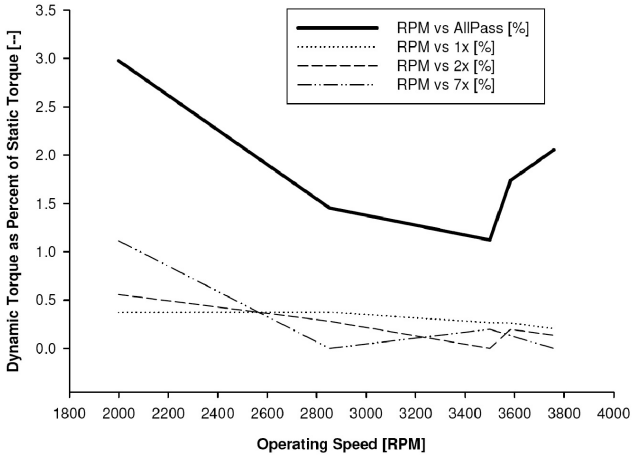

Figure 20. Dynamic Torque Measurements.

Startup and Short-Circuit Transient Excitations

While steady-state excitation sources may, in rare cases, result in torsional problems, the primary concern with fixed-speed units lies with transient excitations (startup, bus-transfer, and short-circuit). Under resonance conditions, the dynamic torque levels associated with (repeated) transient excitation events can result in excessive shaft stresses, shaft breakage, or coupling failures. The maximum dynamic stress amplitude in case of a startup or short circuit event can be in excess of 10 times of maximum static torque (>10 per unit). Torque in electric machines is often expressed as a per unit (PU) value, derived by dividing the actual torque by the corresponding rated (static) torque.

Startup

In contrast to direct-online (DOL) operation, VFDs always incorporate current regulation and limiting functions. During starting, the VFD output frequency starts at a very low value and slowly increases, while the current is controlled to one PU or less. The starting sequence assures that the machine flux is nearly nominal as torque is generated. Therefore the slip is always a small value as the machine accelerates. *This means that the torque is much smoother compared to direct-online starting*. On the other hand, when an induction machine is directly connected to the utility (no VFD), there is a large inrush current, on the order of 5 PU. Initially, the rotor flux is zero, but the stator flux assumes its normal amplitude and angular velocity as the utility voltage is applied. So, due to the large currents, there are very large torque pulsations as the rotor flux slips by the stator flux until equilibrium is attained. The key difference in the VFD operation is that it can adjust both frequency and voltage simultaneously, thus allowing the current and the slip to be carefully controlled during all situations. It is worthwhile to note that thyristor-based solid-state starters can control current during starting but not frequency, so they are not able to produce nearly as smooth a start as a VFD.

Bus Transfer

A particularly bad event for transient torques is bus transfer. In some applications, the motor is switched rapidly from one utility source to another. During the open interval, the motor flux does not

decay much, but the rotor position begins to fall behind where the stator flux will be when reconnected. If reconnection occurs at the wrong time, the inrush currents react with already present flux to create a very, very large torque transient. This must be avoided. If a VFD is present, it will trip when the utility voltage goes to zero, then smoothly restart when the voltage is restored.

Short-Circuit

One feature common to all VFDs (both medium voltage [MV] and low voltage [LV]) is a means of limiting short-circuit current at the output. This is included to prevent a short-circuit in the motor or its cables from damaging the VFD. There are a number of ways to accomplish this. In the current-fed circuits (LCI and symmetrical gate controlled thyristor [SGCT] based), the direct current link filter is an inductor that filters the DC link current. If an external short-circuit occurs, the fault current is strictly limited by the inductor in the short-term, allowing time to phase back the line-side converter and thus extinguish the current. The voltage-fed drives have a more difficult problem, as the DC link capacitor will try to discharge through the output devices and into the short circuit. In the case of those VFDs using insulated gate biploar transistors (IGBTs) the devices are fast enough to turn off when the overcurrent is detected, before any damage is done. Modern IGBTs are inherently current limited to about 3 to 4 PU current, and thus will limit the current even if an overcurrent function does not occur. The voltage-fed drives using IGCTs have a fast detector to initiate a turn-off of the devices if the current gets too high. There is also a small inductor to limit the rate of rise of current to give the detector time to function. In all cases, the response time is short, from tens to a hundred microseconds. Accidental short circuits in the motor terminal box are so common that VFDs must have short-circuit protection. From the motor point of view, if something fails in the VFD, such as a shorted device, the universal response of all VFDs is to turn off all the switching devices, disconnecting the motor so it does not see a short circuit on its terminals. A single shorted device can be prevented from causing large fault currents since the other devices can successfully interrupt the circuit.

Conclusions

Drive protection and slow-start characteristics of VFDs effectively and reliably prevent high torsional stress situations in case of short circuit fault conditions and motor startup. These worst case torsional excitation mechanisms are therefore eliminated when applying a VFD. With the exception of LCI-type VFDs, the steady-state torque harmonic excitation levels induced by state-of-the-art VFD technology results in low and acceptable torsional shaft stresses. Other potential torsional excitation mechanisms such as 1× and 2× running speed and vane-pass frequency excitation also generally result in acceptably low torsional stresses.

It is therefore suggested to consider shaft trains supplied with state-of-the-art VFD technology as torsionally safe and to omit torsional rotordynamic analysis on such shaft trains.

The only exceptions from this rule are LCI-type VFDs where a steady-state torsional analysis investigating the effect of VFD torque harmonics is recommended and, possibly, shaft trains including gearboxes. A standard torsional rotordynamic acceptance criterion requires a minimum of 10 percent frequency separation margin between torsional modes and applicable excitation frequencies. In case of violation of this criterion, detuning of the natural frequency of concern is an option for fixed speed applications only. There, the most commonly applied detuning method implements changes to the coupling torsional stiffness, designed at providing the desired 10 percent separation margin. In case of VFD applications with wide continuous operating speed ranges, critical speed situations are virtually unavoidable, and it is recommended to prove the acceptability of the rotor design by means of forced response analysis investigating the resonance conditions of concern. Chances are high that the steady-state resonance conditions produce acceptably low stresses.

STRUCTURAL DYNAMICS

General

The correct use of analytical and experimental techniques is essential to identifying and solving structural resonance problems. Most centrifugal pumps and their supporting system are too complex to be analyzed with simplified hand-calculation methods. These simple techniques are not discussed in this paper. The presented case studies apply finite element analysis (FEA), the most popular analytical method in use. When choosing the appropriate modeling technique and combined with the necessary level of detail, including application of the correct boundary conditions, FEA can be highly accurate and useful in identifying and resolving resonance conditions. This section also discusses modal analysis as an experimental technique used to identify structural natural frequencies, mode shapes, and recording of operational deflection shapes (ODS). The most accurate and useful results are often obtained when combining analytical and experimental methods.

Horizontal pump structural vibration problems primarily occur at 1× rotational frequency and at vane-pass frequency. Vibration problems at rotational speed frequency typically involve support structure (baseplate, etc.) modes combined with rigid-body motion of the pump casing. The second problem set, with vibrations occurring at vane pass frequency, usually involves bearing housings and sometimes auxiliary piping. Vertical pump structural vibration issues typically occur at running speed frequency or at subsynchronous frequencies, often around 50 percent of rotational speed. In most cases structural vibrations do not become excessive unless amplified by resonance. Structural resonance occurs when the natural frequency of a structure coincides with an applicable excitation frequency like bearing whirl/instability (0.5×), mechanical and hydraulic unbalance (1×), or pressure pulsations at vane-pass frequency.

Structural modes are only lowly damped. Resonance conditions are therefore likely to result in excessive structural vibration levels if properly excited. In case of VFD applications with wide operating speed ranges, chances for resonance conditions to be present are high. It is recommended to predict resonance conditions by means of FEA or modal testing before the pump is installed in the field. Identified resonance conditions should be detuned or avoided. A first case study explains the process of identifying and resolving a horizontal pump baseplate structural resonance problem.

Baseplate Vibration Problems

A multistage, barrel-type 6×8×10.5 CP 13 stage pump operating at 3580 rpm (59.7 cpm) fixed speed in boiler feed-water service, exhibited excessive horizontal bearing housing and casing vibrations. Unfiltered peak vibration levels in the horizontal direction of 1.80 in/sec on the inboard and 1.38 in/sec on the outboard bearing housing were measured. The corresponding peak vibration levels filtered to 1× rotational frequency were 1.60 in/sec and 1.13 in/sec, respectively. Pump vibrations in the vertical direction as well as all motor structural vibrations were acceptably low. A modal finite element analysis simulating a grouted baseplate and rigid pump-casing was performed. Figure 21 presents a plot of a calculated baseplate mode shape with a 62.2 Hz natural frequency. The pump-side is structurally entirely decoupled from the motor-side because of the grouted condition of the baseplate. The mode shape characterized by inboard and outboard pedestals moving in phase with each other was confirmed by modal testing. An impact test performed on both bearing housings revealed amplitude peaks at 62.5 Hz, confirming structural resonance as the root cause of the vibration problem. The result of an impact test performed on the inboard bearing housing in the horizontal direction is presented in Figure 22.

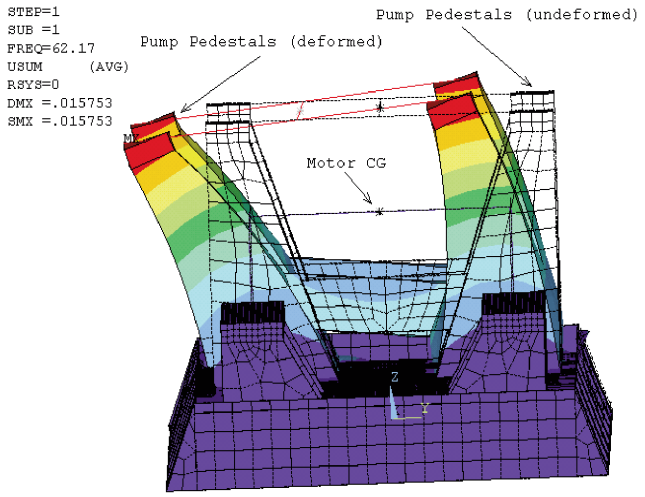

Figure 21. Baseplate Mode Shape.

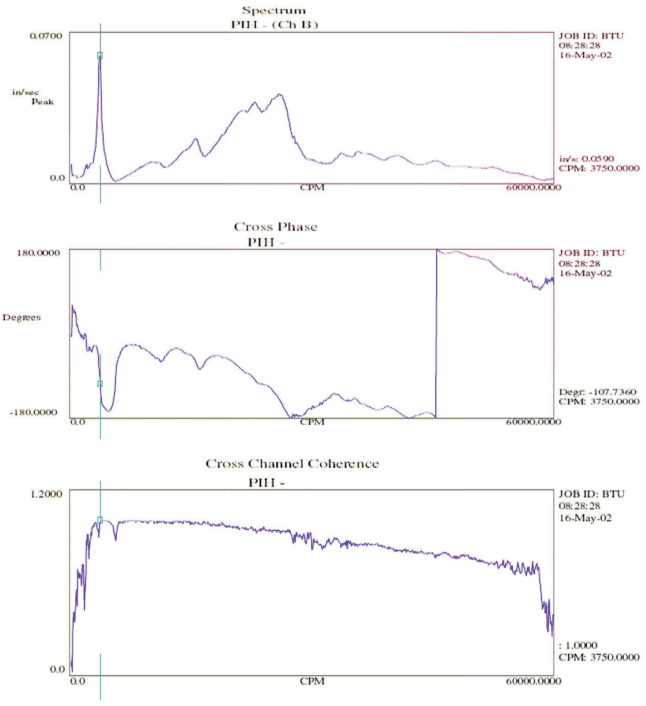

Figure 22. Bearing Housing Impact Test.

The resonance problem could have been resolved by means of reducing the excitation forces or by detuning the structural resonance. The first approach was not recommended in this case because of the acceptably low vibration levels measured in the vertical direction. In case of a structural resonance with a supersynchronous natural frequency, detuning is best done by increasing the stiffness and therefore increasing the structural natural frequency. Various detuning options were analyzed and optimized with FEA. The following is a list of implemented design modifications, depicted in Figure 23:

- Extended the existing C 6 inch × 8.2 lb channels down to the deckplate and added further support in the axial direction by welding on a triangular shaped gusset plate. The two existing C-channels connect the individual pedestals in the horizontal direction.
- Reinforced each pedestal with two short-height outside structural rips
- Added additional side-rail gusset plates

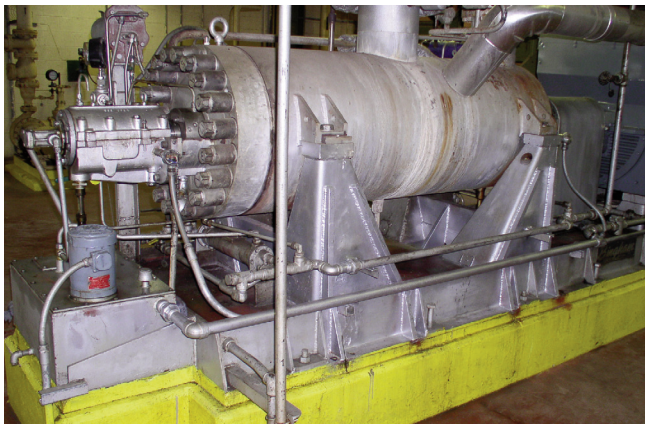

Figure 23. Structurally Modified Baseplate and CP Pump.

Impact tests performed after the modifications indicated that the baseplate natural frequency of concern increased by 8 percent to 67.5 Hz. Unfiltered peak vibration levels dropped by approximately 90 percent to 0.177 in/sec on the inboard bearing housing and 0.112 in/sec on the outboard bearing housing, respectively. Pump vibrations in the vertical direction and all motor vibrations remained low.

The identification of baseplate structural resonances applying FEA is fairly easy and straightforward. The major advantage of the FEA approach is the possibility to perform a reasonably accurate, low-cost analysis in the early phases of a project. Design changes can be implemented before the actual structure is built. Another advantage is the ability to test out design variations and thus optimize the baseplate design on the computer, avoiding modifications of the actually built structure. The most accurate results are usually achieved when combining FEA with modal testing. This approach allows tuning of the FE model to the actually measured natural frequencies and comparison of mode shapes. Obviously a combination of methods is only possible in case the structure is already built and installed.

Not all baseplate structural resonance problems should be overtuned, i.e., detuned by means of reinforcing the structure. In some cases it may be more practical to undertune by adding weight (e.g., filling pedestals with sand or steel pellets, replacing an existing bearing housing with a heavier one, etc.) or cautiously weakening the structure.

Experimental Testing

Two experimental testing methods are shortly discussed. Modal testing allows identification of structural natural frequencies and mode shapes. This type of testing is performed on the standstill machine. The only forces acting are the ones induced by an instrumented hammer or by a shaker. A hammer impact excites the structure over a wide frequency range. This allows measurement of natural frequencies within a desired frequency range. A shaker will excite the structure at a single, specified frequency and is typically applied in a frequency-sweep mode, scanning the structure for structural resonances. The other experimental testing method, operational deflection shape, records structural motion forced by operating loads. ODS measurements illustrate and quantify the parts of the structure that are really moving at a particular frequency due to effectively present excitation. Refer to Richardson (1997) for further information on ODS.

Impact testing is a popular, easy to perform modal testing method that allows measuring of structural natural frequencies. It can be done quickly and rather inexpensively applying an instrumented hammer, a dual-channel fast Fourier transform (FFT) analyzer with postprocessing software, and an accelerometer probe. Structural resonances may be identified by means of a single-channel impact test measuring the response of structure

to a nearby impact. However, the positive identification of a resonance condition requires the use of a dual-channel FFT analyzer. One channel is used to record the impact force and the second channel records the response, typically measured by an accelerometer probe mounted to the structure under investigation. The three individual diagrams in Figure 22 represent amplitude response, cross-channel phase, and cross-channel coherence plots. A resonance condition is not just defined by a peak in the amplitude response spectrum but also by a phase shift. For a single degree of freedom system, the resonance frequency (natural frequency of the system) is accompanied by a 180 degree phase shift. In case of real structures with multiple modes, the phase shift will be less than 180 degrees but still identifiable. Coherence is a measure of how much of the response energy originates from the impact. Valid impact tests have coherence levels close to 100 percent at the resonance frequency. A peak in the amplitude spectrum could be caused by other nearby operating equipment. In such a case, the amplitude peak does not represent a resonance, the phase spectrum is likely to show no significant phase change, and the coherence would be significantly less than one at the corresponding frequency. For further details on modal testing, refer to Ewins (1986).

Baseplates Mounted Onto Flexible Support Structures

Special attention needs to be given to baseplates mounted onto flexible skids or offshore platforms. The flexible substructure acts as an additional spring in series with the baseplate stiffness and therefore influences the baseplate natural frequencies. The case of a 14×14×18.5D MSDD two stage pump mounted on a flexible skid demonstrates the influence of the flexible support structure. The VFD operated pump is in crude oil service with a continuous operating speed range of 2500 to 3960 rpm, which corresponds to a 1× synchronous speed excitation range of 37.5 and 72.6 Hz. The finite element analysis was used to optimize the baseplate and skid design in order to keep the VFD operating speed range free from structural resonance conditions that could be excited by unbalance (1×). Figure 24 illustrates the solid model of the baseplate and flexible skid. The first six structural natural frequencies are listed in Table 1. The middle column lists the natural frequencies for the case of a rigid skid and the column to the right states the same data for the case of a flexible substructure.

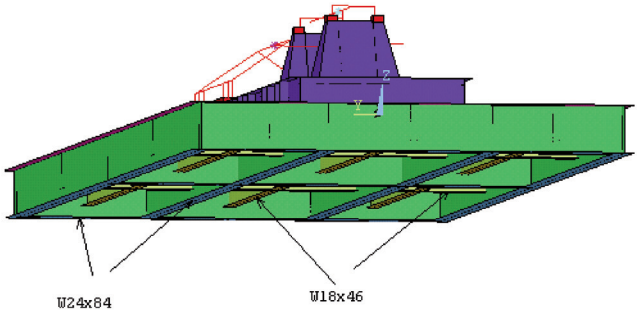

Figure 24. Solid Model of Baseplate and Skid.

Table 1. Calculated Structural Natural Frequencies.

Mode	Natural Frequency [Hz] Rigid Module	Natural Frequency [Hz] Flexible Module
1st Axial	23.9 (100 %)	18.4 (77.0 %)
1st Lateral	44.0 (100 %)	26.3 (59.8 %)
2nd Axial	46.2 (100 %)	27.1 (58.7 %)
1st Vertical	57.3 (100 %)	27.7 (48.3 %)
2nd Lateral	82.1 (100 %)	36.5 (44.5 %)
2nd Vertical	95.6 (100 %)	37.1 (38.8 %)

The case demonstrates the significant influence of the flexible support structure and the usefulness of FEA in the design process.

Bearing Housing Vibration Problems

Horizontal pump bearing housing natural frequencies are typically well above synchronous speed and are therefore not excitable by 1× unbalance excitation. Bearing housing vibration problems often occur at vane pass frequency or multiples thereof. As usual with resonance problems, resolution can be achieved by reducing the excitation source or by detuning the resonance condition. Practical means of reducing the excitation source are described in the previous section excitation sources and amplifiers. This section focuses on the identification of bearing housing natural frequencies and applicable detuning methods. It is possible to calculate bearing housing natural frequencies using FEA but the process is cumbersome and time-intensive. The casing stiffness and the rotor mass acting on the bearing both influence bearing housing dynamics. These influencing factors and the need of an accurate 3D computer aided design (CAD) model of the housing itself make the upfront calculation of bearing housing natural frequencies rather expensive and unpractical.

Bearing housing natural frequencies do not significantly change between test and field installation. Bearing housing impact tests on a test-stand need to be performed on the fully assembled pump, securely mounted onto test pedestals or the actual job baseplate. *It is recommended to impact test bearing housings on a test-stand and avoid resonance situations that could potentially be excited by pressure pulsations at vane-pass frequency*. However, there is no direct correlation between a measured bearing housing natural frequency and the corresponding bearing housing vibrations that occur when operating the equipment at the resonant frequency. In case a pump runs at or near best efficiency point and sufficient B-gap was applied, the resulting pressure pulsation levels may not cause a vibration issue even when operating at resonance conditions.

In order to avoid potential bearing housing vibration problems it is recommended to detune identified bearing housing resonances. The following detuning methods have been successfully applied:

- Reducing of the stiffness of the bearing housing to bearing bracket joint by means of relocating the lower pair of housing bolts as close to the upper pair as possible. Applied to outboard bearing housings, this very effective modification often drops the vertical bearing housing natural frequency by 100 to 150 Hz.
- Alternatively, a stiffness reduction may also be achieved by means of slotting of bearing brackets aimed at reducing the contact area between housing and bracket.
- Changing from a 180 to a 360 degree bearing housing attachment
- Adding weight to the housing (bolted-on or cast-in)
- Providing additional structural support (bracing)

In many cases it is perfectly acceptable to not fully detune a resonance condition but to move it to lower frequencies, excitable at lower operating speeds. Equation (11) indicates that pressure pulsation levels are proportional to the square of the speed.

Vertical Pump Structural Vibration Problems

The process of vertical pump structural analysis is described in the "LATERAL ROTORDYNAMICS" section. Structural modes are lowly damped and resonance situations with 1× and 0.5× synchronous speed should be avoided. Both types of resonance can result in excessive structural vibrations. Detuning options include adding mass, applying seismic supports, and stiffening of driver-stands, columns, mounting plates, or sole plates, etc.

Conclusions

Structural resonance situations with 1× running speed frequency and vane-pass frequency should be avoided in case of horizontal pump applications. With vertical pumps, excitations of concern are at 0.5× and 1× running speed frequency. Structural natural

frequencies and mode shapes can be identified applying FEA and/or modal testing. In case structural resonances cannot be detuned, alternative options aimed at ensuring acceptable operation and vibration performance include:

- Locking out/programming out of specific operating speeds from continuous operation
- Detuning of a resonance to a natural frequency excitable by lower rpm operation. The excitation levels at a lower rpm are likely to be reduced because pressure pulsation amplitudes and unbalance forces both are proportional to the square of speed.
- Reducing the excitation magnitude by means of balancing, increasing B-gap, etc.

ACOUSTIC RESONANCE

General

Acoustic resonance can occur in suction and discharge piping, in the long crossover of multistage pumps, and other fluid filled channels. The phenomenon takes place when the return of a reflected pressure wave, generated by a periodic excitation, coincides with the generation of the next pressure pulse. In that case, a standing wave forms inside the fluid filled channel. Standing waves are acoustic eigenvalues in pipes or piping systems. Acoustic resonance occurs when an acoustic eigenfrequency coincides with an excitation frequency, for example pressure pulsations at vane-pass frequency. The channel length may be equal to quarter, half, or full wavelengths and multiples thereof as illustrated in Figure 25.

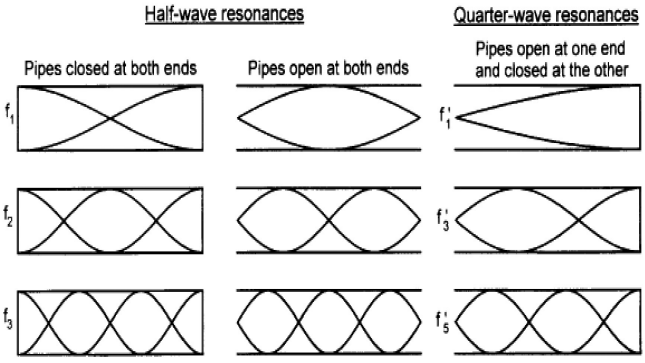

Figure 25. Standing Wave-Forms.

The channel length is determined by a reflective condition at the end of the channel opposite to the induction of the pressure wave. Reflective conditions exist at channel reductions, valves, etc. The reflection at a channel reduction is best explained with acoustic impedance theory. Acoustic impedance Z is a function of the fluid density ρ, the fluid speed of sound c, and the channel cross-sectional area A as defined in Equation (19). Acoustic impedance is a measure of how much a cross-section of a fluid-filled channel resists fluid motion when subject to pressure.

$$Z = \frac{\rho * c}{A} \tag{19}$$

The ratio of reflected to incidental power of a wave hitting a channel reduction is defined in Equation (20). A sketch of a channel reduction is shown in Figure 26.

$$\frac{Power_{Rfl}}{Power_{Inc}} = \frac{(Z_1 - Z_2)^2}{(Z_1 + Z_2)^2} \tag{20}$$

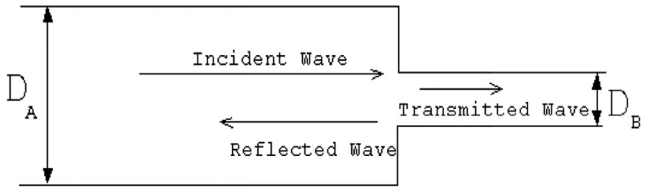

Figure 26. Incidental and Reflected Waves at Channel Reduction.

A 50 percent diameter reduction in a cylindrical channel causes 36 percent of the power of the incident pressure wave to be reflected. In case of an 80 percent reduction ($D_B = 0.2*D_A$), 85 percent of the incident power is reflected. Similarly, an expansion where the pipe diameter doubles, 36 percent of the power of the incident pressure wave is reflected.

A common and most important example of acoustic resonance in centrifugal pumps are long crossover (long crossunder) acoustic resonance in multistage, volute-type pumps of opposed impeller design. *The hydraulic passage length (fluid-filled channel length) extends from the long crossover volute lip, through the long crossover and receiving impeller to the next short crossover volute lip*. Vane-pass frequency pressure pulsations generated by the long crossover entry stage impeller are the driving force.

The wavelength λ is a function of the fluid speed of sound c and the excitation frequency f and is defined in Equation (21). The fluid speed of sound is a function of the fluid density ρ and the adiabatic (or isentropic) bulk modulus K_S as indicated in Equation (22).

$$\lambda = \frac{c}{f} \tag{21}$$

$$c = \sqrt[2]{\frac{K_s}{\rho}} \tag{22}$$

The bulk modulus is a measure of the fluid's resistance to compression. Fluid volume is a function of the applied pressure, the fluid temperature and compressibility, and the initial volume V_0 under atmospheric pressure. Temperature rises under compression, which further increases the pressure. Slow compression of a fluid, allowing full dissipation of the generated heat, leads to the measurement of an isothermal (constant temperature) bulk modulus. An adiabatic (or isentropic) bulk modulus is measured when compressing the fluid rapidly and measuring pressure due to compression and thermal expansion. The adiabatic bulk modulus should be used for this consideration. The bulk modulus is defined as the slope of the volume versus pressure curve as illustrated in Figure 27. The slope may be defined as a secant, drawing a line from the origin (V_0) to a point on the curve or it can be defined as a tangent at a specified point on the curve, leading to the definition of the secant bulk modulus K_S shown in Equation (23) and the tangent bulk modulus K_T in Equation (24), respectively. Figure 27 illustrates the two definitions.

$$K_s = \frac{V_0}{V_0 - V_1}(P_1 - P_0) \tag{23}$$

$$K_T = V_0 \frac{dP}{dV} \tag{24}$$

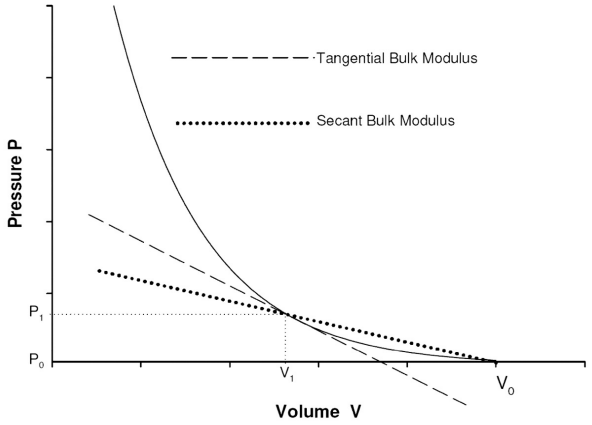

Figure 27. Secant and Tangential Fluid Bulk Modulus.

The stiffness of the pipe or channel structure also influences the fluid speed of sound. For a cylindrical channel of diameter D, wall thickness t, and made out of a material with Young's modulus of elasticity E and density ρ, the effective speed of sound c_1 is defined in Equation (25).

$$c_1 = \frac{c}{\sqrt[2]{1 + \frac{D*\rho*c^2}{t*E}}} \quad \textbf{(25)}$$

Table 2 states approximate speed of sound values for some commonly pumped fluids. The values for diesel, kerosene, and gasoline can vary, mainly because of differences in chemical composition.

Table 2. Approximate Fluid Speed of Sound Values.

Fluid	Density ρ [kg/m³] (Lb/ft³)	Bulk Modulus K_S [N/m²] (psi)	Speed of Sound c [m/sec] (ft/sec)
Water	1000 (62.4)	2.20E9 (3.19E5)	1,480 (4,870)
Diesel	850 (53.1)	1.46E9 (2.12E5)	1,310 (4,300)
Kerosene	810 (50.6)	1.30E9 (1.88E5)	1,265 (4,150)
Gasoline	736 (45.9)	0.96E9 (1.37E5)	1,142 (3,745)

The available (system) damping that limits pressure pulsations is typically low. Structural vibrations caused by acoustic resonance can therefore easily reach damaging levels. In case of long crossover acoustic resonance, bearing housing rms vibrations at vane-pass frequency in excess of 1.0 in/sec (25.4 mm/sec) have been measured.

Case Study—Multistage Pump
Long Crossover Acoustic Resonance

The identification and cure of long crossover acoustic resonance are explained on the example of a 6×8×11J MSD2 multistage pump in pipeline service, pumping batches of diesel, kerosene, and gasoline. The pump initially operated at 3560 rpm and was later converted to VFD operation with an operating speed range of 2000 to 3960 rpm. The pump was fitted with seven-vane impellers. Operation at 3560 rpm indicated highly product dependant vane-pass vibration levels in the vertical direction of the inboard bearing housing. The corresponding filtered (vane-pass frequency) rms vibration levels were 0.06 in/sec for gasoline, 0.42 in/sec for kerosene, and 0.66 in/sec for diesel, indicating a resonance condition.

The theoretical identification of long crossover acoustic resonance is best done applying an acoustic resonance (AR) diagram, plotting the hydraulic passage length together with the frequency dependant wavelength curves. *Acoustic resonance occurs at the intersection between these lines*. The AR diagram is the acoustic resonance equivalent of a Campbell diagram used in lateral and torsional rotordynamics. Figure 28 presents the AR diagram for the above described pipeline pump and the case of a seven-vane impeller at long crossover entry stage. The figure also indicates the increased chance of encountering acoustic resonance when converting from fixed speed operation to VFD operation.

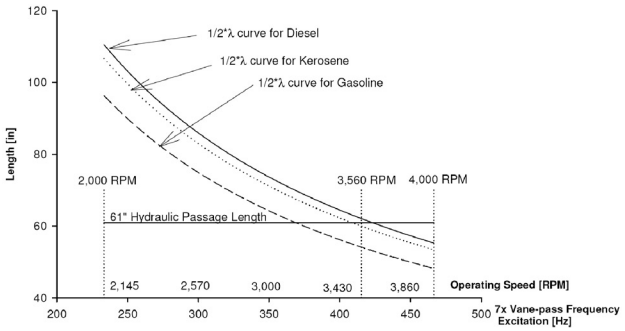

Figure 28. Acoustic Resonance Diagram (7×).

The AR diagram shows resonance conditions associated with the three products. The diesel and kerosene resonances occur close to 3560 rpm operating speed, at approximately 3625 rpm and 3495 rpm, respectively. This explains the high vane-pass vibration levels when pumping these two products.

A first corrective measure applying a 30 degree angle cut-back to both long crossover/crossunder volute lips, resulted in a scissoring effect between the impeller vane twist angle and the volute cutwater. This measure has a tendency to "smear-out" the pressure pulse and also increases the B-gap between impeller and volute. As a result, the rms vane-pass vibration levels dropped from 0.66 in/sec to 0.45 in/sec for diesel pumped at comparable operating conditions. This drop in vibration level, achieved by means of reducing the excitation forces, was not sufficient and the acoustic resonance condition needed to be detuned. The AR diagram for the case of a five-vane impeller installed at the long crossover entry stage is presented in Figure 29. The reduced excitation frequency resolved the resonance condition for all products and over the entire continuous VFD operating speed range.

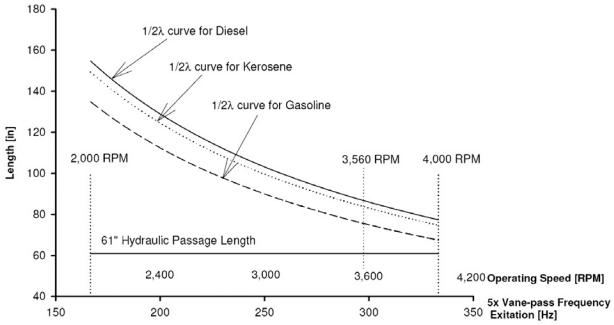

Figure 29. Acoustic Resonance Diagram (5×).

The vane-pass vibration levels measured in the vertical direction of the inboard bearing housing dropped to acceptable levels after implementing this second corrective measure. The gasoline levels were 0.005 in/sec rms 5× and 0.013 in/sec rms 7×, kerosene showed 0.007 in/sec rms 5× and 0.019 in/sec rms 7× levels, and diesel was at 0.007 in/sec rms 5× and 0.016 in/sec rms 7×, respectively.

Corrective Measures

The preferred corrective measures are the ones that detune acoustic resonance conditions, providing a minimum of 10 to 20 percent of separation margin between wavelength curves and the hydraulic passage length line. The following detuning features apply for long crossover acoustic resonance:

- Changing of the vane count of the impeller feeding the long crossover. This changes the excitation frequency and therefore the wavelength λ.

Table of Contents

- Rearranging the destaging arrangement in case of destaged pump. Destaging the impeller at long crossover exit increases the hydraulic passage length.
- Locking out of speed ranges from continuous operation

In case of large continuous operating speed ranges, a resonance condition near maximum speed may be eliminated at the price of creating a new resonance at the lower end of the speed range. This approach may be perfectly acceptable because pressure pulsation levels are proportional to the square of the speed (refer to Equation [11]).

If detuning is not feasible, the applicable excitation levels can be reduced by means of implementing the measures listed below. These modifications do not eliminate the resonance condition and some vane pass vibrations may still exceed the maximum allowable levels. These corrective measures only apply to the impeller feeding the long crossover because it is the driver of long crossover acoustic resonance.

- Cutting back of the crossover and crossunder volute lips in a 30 degree to 45 degree angle, resulting in a "scissoring" effect with impeller vane twist angle. This, together with increasing the B-gap, is the most effective measure reducing excitation levels.
- Minimizing the long crossover volute cutwater thicknesses, providing a "bullet-nose" type profile
- Minimizing the impeller vane outlet thicknesses of the long crossover entry stage impeller by means of overfiling
- Reduction of the shroud thickness at the impeller periphery by means of chamfering
- Providing the long crossover entry stage impeller with extra trim (increasing the B-gap)
- Operation close to BEP/avoiding of part-flow operation

Conclusions

Acoustic resonance in pumps can cause high bearing housing vibrations and also adversely affect casings and baseplates. These amplified structural vibrations can result in auxiliary piping, instrumentation, and bolting fatigue failures. Acoustic resonance is also a source of excessive structureborne noise. The likelihood of encountering acoustic resonance is greatly increased when opening up the continuous operating speed range by applying a VFD. Chances of encountering resonance conditions are further increased when pumping multiple products with different speeds of sound. Upfront identification of potential acoustic resonance condition is recommended and fairly easy when applying an AR diagram. The main difficulties are the identification of the correct hydraulic passage length and the applicable fluid speed of sound value. If necessary, the pump OEM can provide the passage length. In case of a multistage opposed-impeller centrifugal pump, the applicable hydraulic passage length is well defined and the acoustic resonance check can be performed in the tendering or design stage of an order. The channel length in suction and discharge piping may be less clearly defined and special care is required when calculating lengths.

It is recommended to perform a long crossover acoustic resonance check in all cases of VFD operated multistage opposed-impeller centrifugal pumps applying an AR diagram. Resonance conditions should be detuned if at all possible.

MEDIUM VOLTAGE VARIABLE FREQUENCY DRIVES

General

This section presents technical background on commercially available VFDs suitable for operating an induction or synchronous, standard polyphase alternating current (AC) motor at medium voltage (2300 V to 13.8 kV).

Despite the diversity of power circuits, there are two common properties of these drives:

- All of them accept commonly available AC input power of fixed voltage and frequency and, through switching power conversion, create an output of suitable characteristics to operate a particular type of electric machine, which means that they are machine specific. The authors will limit their discussion to those suitable for induction and synchronous motors.
- All of them are based on solid-state switching devices. The development of new devices is the most important driver of VFD technology.

Figure 30 shows the basic structure of most common AC drives. There is an input conversion circuit that converts the utility power into DC, and then an output inversion stage that changes the DC back into variable AC.

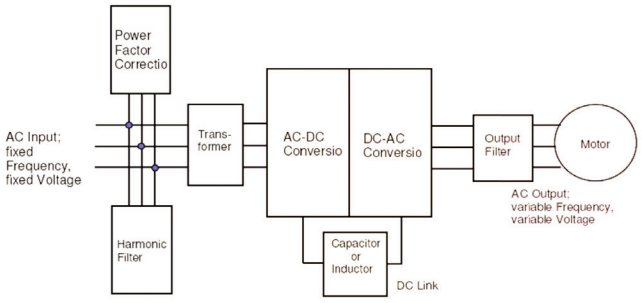

Figure 30. General Structure of a VFD.

Applying VFDs offers a variety of benefits:

- Energy savings where variable flow control is required; variable speed operation replaces wasteful throttling controls
- Optimization of rotating equipment performance
- Elimination of gears or other power transmission devices by matching the base speed of the motor to the driven load
- Automation of process control by using the VFD as the final control element, leading to more efficient part-load operation
- Reduction of the rating and cost of the electrical distribution system by eliminating motor starting inrush
- Extension of motor, bearing, and seal life
- Reduction of noise and environmental impact. Electric drives are clean, nonpolluting, quiet, efficient, and relatively easy to repair.

Development of Semiconductor Switching Devices

VFDs became practical after the invention of the thyristor in 1957. Table 3 shows a comparison of the properties of devices commonly in use today.

Table 3. Semiconductor Switching Devices.

Device Type	Maximum Available Blocking Voltage	Maximum Available Current	µsec Off Time (typical)	Peak Gate Power	ON State Voltage	Relative Cost
Diode	10000	10000	50	N/A	1.0	Low
Thyristor	10000	10000	25-300	3 W	1.2	Low
Transistor	1500	1800	3-5	20 W	2	Medium
IGBT	6500	2400	0.5	3 W	3-5	Medium
IGCT	6500	4000	2-3	45 KW	1.5-2.5	Med-High
SGCT	6500	4000	2-3	45 KW	2-3	Med-High

The thyristor (silicon controlled rectifier type, SCR) is a four-layer (one thin disc of silicon with four layers of different properties) semiconductor device that has many of the properties of an ideal switch. It has low leakage current in the off-state, a small voltage drop in the on-state, and takes only a small signal to

initiate conduction (power gains of over one million are common). When applied properly, the thyristor will last indefinitely. After its introduction, the current and voltage ratings increased rapidly. Today it has substantially higher power capability than any other solid-state device but no longer dominates power conversion in the medium and higher power ranges. The major drawback of the thyristor is that it cannot be turned off by a gate signal, but the main current must be interrupted in order for it to regain the blocking state. The inconvenience of having to commutate (turn off) the thyristor in its main circuit at a very high energy level has encouraged the development of other related devices as power switches.

Transistors predate thyristors, but their use as high-power switches was relatively restricted (compared with thyristors) until the ratings reached 50 A and 1000 V in the same device, during the early 1980s. These devices are three-layer semiconductors that exhibit linear behavior but are used only in saturation (fully turned on) or totally off. In order to reduce the base drive requirements, most transistors used in VFDs are Darlington types (a tandem arrangement in which there are two transistors, the first one feeding the base input of the second). Even so, they have higher conduction losses and greater drive power requirements than thyristors. Nevertheless, because they can be turned on or off quickly via base signals, transistors quickly displaced thyristors in lower drive ratings, and were once widely used in pulse-width modulated inverters. They in turn were displaced by insulated gate bipolar transistors in the late 1980s. The IGBT is a combination of a power bipolar transistor and a metal-oxide semiconductor field-effect transistor (MOSFET) that combines the best properties of both devices. A most attractive feature is the very high control input impedance that permits them to be driven directly from lower power logic sources. Their power handling capability has increased dramatically and they are now viable alternatives to thyristors and integrated gate controlled thyristors in the largest drive ratings.

It has long been possible to modify thyristors to permit them to be turned off by a negative gate signal. These devices are four-layer types and are called gate-turn-off thyristors, or simply GTOs. These devices have been around since at least 1965, but only in the mid 1980s did their ratings increase to high power levels. Present-day GTOs have about the same forward drop as a Darlington transistor (twice that of a conventional thyristor). GTOs require a much more powerful gate drive, particularly for turn-off, but the lack of external commutation circuit requirements gives them an advantage over thyristors. GTOs are available at much higher voltage and current ratings than power transistors. Unlike transistors, once a GTO has been turned on or off with a gate pulse, it is not necessary to continue the gate signal because of the internal positive feedback mechanism inherent in four-layer devices. Unfortunately, high cost and very large switching losses restricted the use of GTOs to only those applications in which space and weight were at a premium. In 1997 the IGCT was introduced. This is very similar in construction to the GTO, but a new method of turn-off and special metallurgy has resulted in a device considerably better than the GTO in forward drop and switching losses. It has a sibling, the symmetrical gate controlled thyristor (SGCT), which has similar properties but can also block reverse voltage, which the IGCT cannot. Voltage-fed circuits use IGCTs while current-fed circuits need SGCTs.

Today the thyristor, IGBT, SGCT, and IGCT form the technological base on which the solid-state variable speed drive industry rests. There are other device technologies and enhancements in various stages of development that may or may not become significant depending on their cost and availability in large current ratings (> 50 A and a voltage rating of at least 1000 V). These include: trench gate construction for IGBTs, silicon carbide semiconductors, variants of the four layer switch such as the MTO (MOS turn-off thyristor), and MCT (MOS controlled thyristor). New switches are expected to come along and significantly improve on the devices currently in use. While the type of semiconductor device should not be the most important issue to a user, in general the newer devices provide better drive performance.

Drive Control Technology

Parallel to the development of power switching devices, there have been very significant advances in hardware and software for controlling VFDs. These controls are a mixture of analog and digital signal processing. The advent of integrated circuit operational amplifiers and integrated circuit logic families made dramatic reductions in size and cost of the drive control possible, while permitting more sophisticated and complex control algorithms without a reliability penalty. These developments occurred during the 1965 to 1975 period. Further consolidation of the control circuits occurred after that as large-scale integrated circuits (LSI) became available. In fact, the pulse-width modulation control technique was not practical until the appearance of LSI circuits because of the immense amount of combinatorial logic required. Clearly, the most significant advance in drive control has been the introduction of microprocessors into drive control circuits. The introduction of cheap and powerful microprocessors continues to expand the capability of drive controls. A modern drive should have most of these features. The performance enhancements include:

- More elaborate and detailed diagnostics owing to the ability to store data relating to drive internal variables, such as current, speed, firing angle, etc. The ability to signal to the user if a component has failed.
- The ability to communicate both ways over industry standard protocols with the user's central computers about drive status.
- The ability to make drive tuning adjustments via keypads with parameters such as loop gains, ramp rates, and current limits stored in memory rather than potentiometer settings.
- Self-tuning and self-commissioning drive controls.
- More adept techniques to overcome power circuit nonlinearities.

AC Variable Frequency Drives

The effect of new solid-state switching devices was very significant on AC variable speed drives, and it shows no sign of stopping. AC drives are machine specific and more complex than DC drives, mostly because of the simplicity of the AC machine. Solid-state VFDs have been developed and marketed for wound-rotor induction motors (WRIMs), cage-type induction motors (IM), and synchronous motors.

Historically, WRIM-based VFDs were in common use long before solid-state electronics. These drives operate on the principle of deliberately creating high-slip conditions in the machine and then disposing of the large rotor power that results. This is done by varying the effective resistance seen by the rotor windings. The WRIM is the most expensive AC machine. This has made WRIM-based variable speed drives noncompetitive as compared with cage induction motor drives or load commutated inverters using synchronous machines. The slip (s) is defined as the ratio of the difference between the stator flux angular velocity and the rotor angular velocity, to the stator flux angular velocity.

$$s = (\omega_S - \omega_R) / \omega_S \quad \textbf{(26)}$$

Thus when a machine is operating at a speed less than that of the stator flux (determined by the stator voltage frequency and the pole number), it is slipping. That is not necessarily bad, but of the total power flowing across the air-gap into the rotor, the fraction s is lost as heat in the rotor, and (1-s) comes out of the shaft as useful mechanical power.

Induction Motor Variable Speed Drives

Because the squirrel cage induction motor is the least expensive, least complex, and most rugged electric machine, great effort has gone into drive development to exploit the machine's superior qualities. Owing to its very simplicity, it is the least amenable to variable speed operation. Since it has only one electrical input port, the drive must control both flux and torque simultaneously through this single input. As there is no access to the rotor, the power dissipation there raises its temperature and therefore very low-slip operation is essential. Induction motor VFDs in the past have had the greatest diversity of power circuits. Today, for induction motor MV drives rated 2300 V and up, there are essentially only two main choices:

- The IGBT/IGCT voltage-fed pulse-width modulated drive. In this type of voltage source inverter both the frequency and amplitude are controlled by the output switches alone. A representative circuit based on IGBTs is displayed in Figure 31. This shows the conceptual design, but as indicated is used for VFDs operating at less than 1000 V. The input converter is a diode bridge so that the DC link operates at a fixed unregulated voltage. The diode front end gives close to unity power factor, independent of load and speed. This type of drive is called pulse-width-modulated because the output voltage waveform is synthesized from constant amplitude, variable-width pulses at a modest (200 to 1200 Hz) frequency so that a sinusoidal output is simulated. The lower (voltage) harmonics (five, seven, 11, 13, 17, 19, etc.) are not present in modern PWM drives. One advantage is smooth torque, low output harmonic currents, and no cogging (cogging is visible jerky rotation at low speed caused by large harmonic currents). Although this approach eliminates the phase control requirements of the thyristor converter, it requires fast output switches. Since every switching event causes an energy loss in the output devices, fast switches are needed in order to support a high switching frequency without excessive losses in the output switches. Occasionally, high-frequency switching may cause objectionable acoustic noise in the motor, but that has been overcome with special modulation techniques and higher switching frequencies (3000 Hz and up). There are IGBT PWM VFDs on the market today in the range of 1 kW to 1 MW at 460, 600, and 690 VAC rated input. As with all voltage source inverters fed by diode rectifiers, regeneration of power to the line is not possible. The voltage-fed PWM MV drive is available in two subtypes: The neutral-point clamped circuit, and the series cell multilevel circuit.

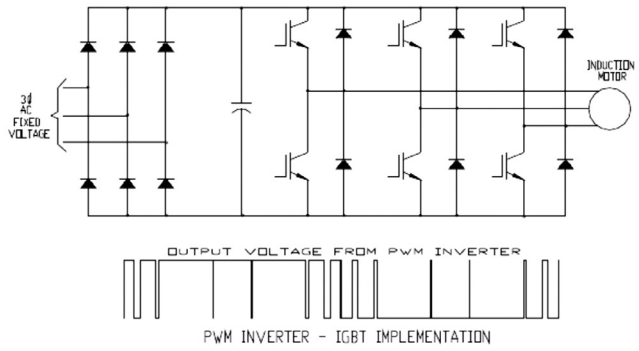

Figure 31. Low-Voltage PWM Drive Illustrating Voltage-Fed PWM Technology.

- The SGCT based current-fed pulse width modulated drives (refer to Figure 33 for example). In this type of current source inverter only the frequency is controlled by the output switches. The input converter is a thyristor bridge so that the DC link operates at a variable controlled voltage, and with the link inductor, functions as an adjustable current source. The thyristor front end gives a variable input power factor, dependent on load and speed. Ordinarily, this drive would produce an output like the LCI, that is 120 degrees square pulses of current separated by 60 degree intervals of zero current. But, since there must be a capacitor bank at the output, the motor current has improved waveform due to the capacitors absorbing some of the harmonics. Furthermore, this type of drive generally also uses a form of pulse-width-modulation. The 120 degree output current pulses are subdivided into several narrower width pulses interspersed with short intervals of zero current. This technique suppresses the lowest-order (current) harmonics (five, seven, etc.) Since every switching causes an energy loss in the output devices, fast switches are needed in order to support a high switching frequency without excessive losses in the output switches. Due to the output capacitor filter, acoustic noise in the motor is not an issue.

Current-Fed Versus Voltage Fed Circuits—
The Two Basic Topologies

The terms voltage-fed and current-fed refer to the two basic VFD strategies of applying power to the motor. In Europe, these are called voltage-impressed and current-impressed, which is a clearer description.

In voltage-fed circuits, the output of the inverter is a voltage, usually the DC link voltage. The motor and its load determine the current that flows. The inverter does not care what the current is (within limits). Usually, these drives have diode rectifiers on the input. The main DC link filter is a capacitor.

In current-fed circuits, the output of the inverter is a current, usually the DC link current. The motor and its load determine the voltage. The inverter does not care what the voltage is. Usually these VFDs have a thyristor converter input stage, and the DC link element is an inductor.

Table 4 states a summary comparison of the properties of the two types of VFDs.

Table 4. Comparison of Current-Fed and Voltage-Fed Drives.

Current-fed type VFD	Voltage-fed type VFD
Lower cost at higher horsepower	Lower cost at low horsepower
Four-Quadrant	Two-Quadrant
P.F. = P.U. Speed*Load P.F.	95 % displacement P.F.
96.5 % efficiency	96 to 97.5 % efficiency
Immune to short circuits	Requires protection for short circuits
More low-cost components	Few higher-cost components
Large inductors (bulky and costly)	Small- or no inductors
Lower motor noise	Low to medium motor noise
Non-critical layout	Critical construction layout
30 % harmonic current (6-P)	40 % harmonic current (6-P)
Low dV/dt at output	High dV/dt at output
High common-mode voltage	Low common-mode voltage
Output filter required	Output filter not needed

Medium-Voltage Variable Frequency Drives

For drives rated 2300 VAC and above on the output, there are a number of choices of design of both current- and voltage-fed types:

- The load commutated inverter
- The current-fed SGCT inverter
- The neutral-point-clamped inverter
- The multilevel series cell VFD

The Load Commutated Inverter

As illustrated in Figure 32, the load-commutated inverter is based on a synchronous machine. All the thyristors are naturally commutated (natural commutation is the turn-off process of a thyristor when a sinusoidal voltage source in the circuit applies reverse voltage to the device), because the back electromagnetic field (EMF) of the machine commutates the machine-side converter. The machine-side converter operates exactly like the line-side converter, except the phase back angle is about 150 degrees. The machine naturally applies reverse voltage to an off-going device before the next thyristor is gated. This imposes some special design criteria on the synchronous motor, which

includes operation at a substantial leading power factor over the speed range, requirement for sufficient leakage inductance to limit the thyristor di/dt, and ability to withstand harmonic currents in the damper windings. The LCI uses two thyristor bridges, one on the line-side and one on the machine-side. The requirement for the machine to operate with a leading power factor, typically 90 percent, requires somewhat more field excitation and a special exciter compared with that normally applied to synchronous motor. This also results in a 10 percent reduction in the torque for a given current. The machine-side devices are fired exactly synchronized with the rotation of the machine, so as to maintain constant torque angle and constant commutation margin (the time available to turn off a thyristor). This is done either by rotor position feedback or by phase control circuits driven by the machine terminal voltage. Only resistor-capacitor (RC) networks for voltage sharing are necessary. The output current is very similar in shape to the input current, i.e., quasi square-wave, which means a substantial harmonic component. The harmonic currents cause extra losses in the damper bars, and they give rise to very significant torque pulsations. The drive is not self-starting due to the low machine voltage at low speeds that cannot commutate the thyristors. Therefore, the drive is started by interrupting the DC link current with the line-side converter in order to commutate the inverter thyristors. The line-side converter is regulated to control torque. A choke is used between converters to smooth the link current. Load commutated inverters came into commercial use about 1975 and are used mainly on very large medium voltage drives (1 MW to 100 MW). At these power levels, multiple series devices are employed (typically four at 4000 V input), and conversion takes place directly at 2.4 or 4 kV or higher. The efficiency is excellent, and reliability has been very good. Although they are capable of regeneration, LCIs are rarely used in four quadrant applications because of the difficulty in commutating at very low speeds where the machine voltage is negligible. Operation above line frequency is straightforward.

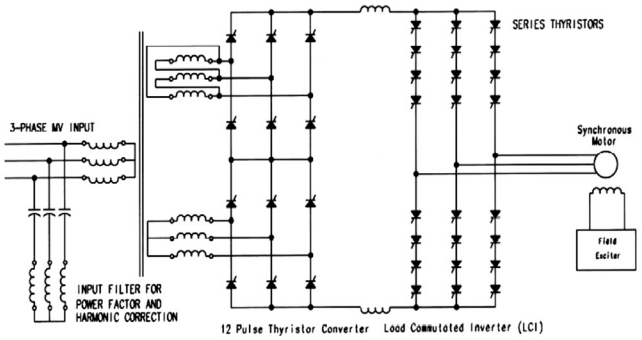

Figure 32. Load-Commutated Inverter with 12-Pulse Input.

Despite the need for special synchronous motors, the LCI drive has been very successful, particularly in very large sizes, where only thyristors can provide the necessary current and voltage ratings. Also, high speed LCIs have been built. Now that self-commutated VFDs are available, the LCI is becoming less popular.

The Current-Fed SGCT Inverter

Another medium-voltage bridge inverter circuit is displayed in Figure 33. Here the output devices are SGCTs (two or three 6.5 kV units per leg will be required) that can be turned off (as well as on) via the gate. There must be a capacitor filter on the output rated about 0.3 PU kVAR. Since the motor appears to be a voltage source behind the leakage reactance, it is not possible to commutate the current between motor phases without a voltage to change the current in the leakage inductance. When an SGCT turns off, there must still be a path for the current trapped in the motor leakage inductance, which is provided by a capacitor bank. The capacitors resonate with the motor leakage inductance during the transfer of current. The choice of capacitor is determined by the permissible ring-up voltage during commutation. All current-fed VFDs with self-commutating switches have the need of a "buffering" capacitor between the impressed current of the inverter and the inductance of the motor. Furthermore, if the capacitor bank exceeds 0.2 PU, the possibility of self-excitation of the motor exists, necessitating a contactor between machine and drive. Voltage-fed circuits do not require these elements, because one can arbitrarily change the voltage across the leakage inductance.

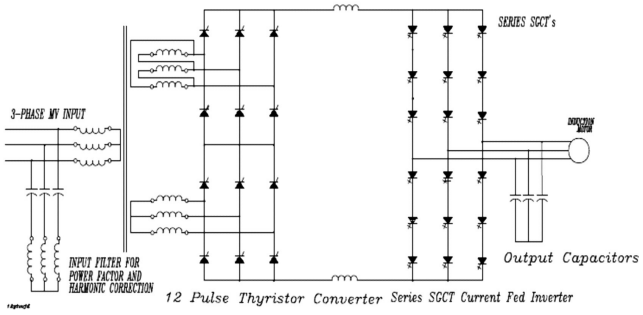

Figure 33. SGCT Current-Fed MV VFD with 12-Pulse Input.

Since the capacitor bank provides some filtering of the output current, the quasi-square wave from the SGCTs does not reach the motor. Most of the high-frequency components are absorbed by the capacitors. Further motor current improvements are made by harmonic elimination switching patterns for the SGCTs. At low frequencies, many pulses per cycle are possible and harmonic elimination is quite effective. But the SGCT frequency limit of a few hundred Hertz restricts harmonic elimination at rated frequency to the fifth and maybe the seventh harmonic.

This frequency limit comes about due to the nature of the SGCT turn-off (and to a lesser extent, turn-on) mechanism. The device is turned off by applying a negative current to gate that is larger than the anode current, over a period of a few microseconds and interrupting the regenerative turn-on mechanism. There is a short period during which the device experiences extremely high internal power dissipation. This is the source of switching losses that have to be considered in the thermal management of the device.

The SGCT gate driver, in addition to providing a turn-on pulse comparable to the thyristor driver, needs to be able to deliver a peak negative current of more than 100 percent of the main current in order to turn off the device. Thus, the SGCT driver has a peak VA rating of two to three orders of magnitude higher than that for a thyristor, and perhaps 10 times the average power requirement. This is an important factor in that all the gate power must be delivered to a circuit floating at medium-voltage potential.

The Neutral-Point-Clamped Inverter

Figure 34 illustrates such a circuit, the neutral-point-clamped inverter. There have been many VFDs of this type applied at 3300 V output with 4.5 kV GTOs, but the circuit has only recently been extended to 4 kV probably due to the improved properties of the IGCT. In the newer versions of this drive, the GTOs are replaced with IGCTs. These devices are similar in construction to a GTO, but are turned off quickly (one microsecond) by drawing all the anode current out through the gate, so that the turn off gain is unity. This requires a higher current gate driver, but lower average power requirements since the turn-off time is so short. The main improvement is that the IGCT can operate with a very small or no snubber (resistor-capacitor [RC] electrical circuit suppressing electrical voltage transients).

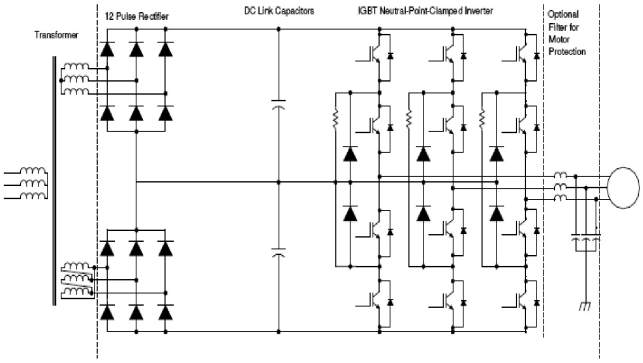

Figure 34. Neutral-Point Clamped MV VFD-IGBT Version with 12-Pulse Input.

In this 4 kV output design, the total DC link voltage is 6 kV, with a midpoint established at the center of the capacitor filter. Each leg of the bridge consists of two 6.5 kV IGCTs in series. There are diodes in reverse across each IGCT to permit motor current to flow back to the link, and still more diodes (same voltage rating as the IGCTs) connecting the midpoints of the inverter legs back to the midpoint of the DC link. The total device count is 12 IGCTs and 18 diodes. The neutral-point-clamped inverter offers several advantages in those cases where series devices would be necessary anyway. First, the clamping diodes permit another voltage level, the DC link midpoint, at the output. This cuts the voltage step seen by the motor in half, and more important, creates another degree of freedom in eliminating output harmonics. Also, the clamping diode positively limits the voltage across any one device to half the link voltage, enforcing voltage sharing without additional RC networks.

Since the switching devices in this circuit are never subjected to reverse voltage, it is preferable to use asymmetrical devices in which the lack of reverse blocking capability is traded off for lower conduction and switching losses (SGCTs are IGCTs that have reverse voltage blocking capability, as required by the current-fed circuit).

Device protection during a short circuit can be a problem, as the IGCT can carry almost unlimited fault current like a thyristor. Unlike the current-fed circuits where fault current is limited, in the voltage-fed circuit, the DC link capacitor can source very large fault currents in the event of a short or a commutation failure. Protection schemes generally attempt to detect the onset of fault current and turn off the devices before it grows beyond the safe turn-off level. It is also possible to use the NPC topology with IGBTs as the switching devices. Although IGBTs are currently available at 6.5 kV, the IGBT NPC is more often constructed of series IGBTs rated 3300 V to reach 4 kV output. The concept of NPC can be extended to M-level inverters, although the number of diodes grows rapidly. Since each device is topologically unique, adding redundant devices would require twice as many, instead of just one more.

The Multilevel Series-Cell Inverter

The patented series cell arrangement of Figures 35 and 36, also known as the perfect harmony drive, addresses the previously mentioned design issues in a unique way. Since there are no devices in series, only series cells, the problem of voltage sharing among series devices is not present. The rectifier diodes and the IGBTs are both closely coupled to the DC link capacitor in the cell and thus cannot be exposed to more than the bus voltage, regardless of the load behavior. Since there is no DC link choke, a voltage transient on the AC mains is converted into a current pulse by the relatively high leakage reactance of the transformer secondary, and does not add to the voltage seen by the diodes.

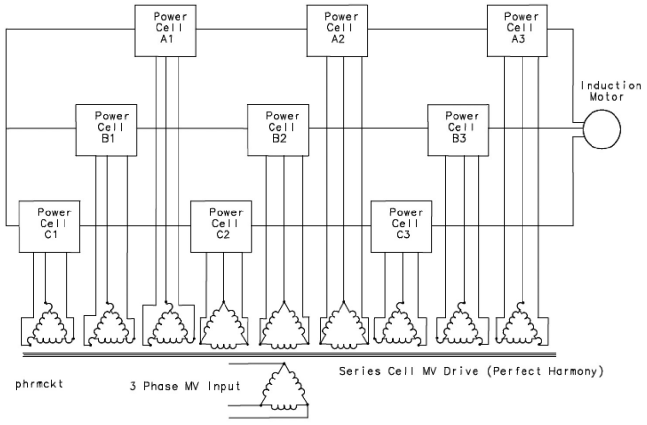

Figure 35. Multilevel Series Cell PWM Drive.

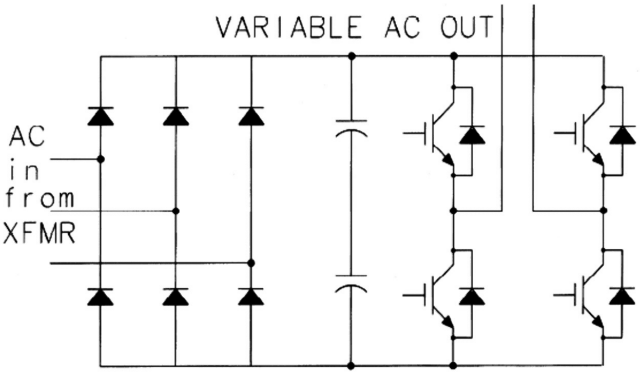

Figure 36. Power Conversion Module Used in Series-Cell Multilevel VFD.

Each cell generates the same AC output. The fundamentals are equal in magnitude and in phase, but the carrier frequency is staggered among the cells in a particular phase. Although an individual cell operates at 600 Hz (or more), the effective switching frequency at the motor is twice the carrier frequency times the number of cells per output phase. This low switching frequency and the excellent high frequency characteristics of the IGBT has the advantage that the IGBT switching losses are very small. The devices can switch well above rated current without the need for snubbers, which also helps in maintaining excellent efficiency. Waveform quality is unaffected by speed or load. For the five cell/phase VFD, there are 10 930 V steps between the negative and positive peaks. With this technique, the concern for high dv/dt on the motor windings is largely avoided.

A major advantage of the IGBT over all other power switches is the extremely low gate power required. The peak power is about 5 W with an average of much less than 1 W. This dramatically simplifies the delivery of gate power compared to the GTO/IGCT. Although there are more active devices in the perfect harmony (60 IGBTs and 60 diodes in the inverter sections) than in the other circuits, the elimination of snubbers, voltage sharing networks, and high power gate drivers compensates for the additional switching devices. The type of IGBTs employed are third and fourth generation isolated base modules, generally the same mature product as those found in 460 VAC and 690 VAC LV PWM drives, and are also used in traction applications. The IGBTs are protected by an out-of-saturation detector circuit that augments the built-in current limiting behavior. Since the cells are assembled into a nonconducting framework and are electrically floating, the mounting and cooling of the IGBTs are no more complex than in a low voltage PWM drive. It is possible to put redundant cells in the string, and also to operate at reduced output with one or more cells inoperative.

Comparison of Medium-Voltage Motor Drives

All the types of drives mentioned above are capable of providing highly reliable operation at a justifiable cost, and have been proven in service. They all have efficiencies above 95 percent. The most significant differences among them have to do with power quality, that is, how close to a sinewave is the input current, and how well does the output resemble the sinusoidal utility voltage. Table 5 compares them on a number of different factors. Note that the voltage-fed drives have an advantage in input harmonics and power factor, and the drives, which do not use thyristors, have a wider speed range.

Table 5. Comparison of Medium Voltage VFDs.

	Load Commutated Inverter	Neutral Point Clamped Inverter	SGCT Current-Fed Inverter	Multilevel Series-Cell Inverter
Switching Device	Thyristor	IGBT or IGCT	SGCT	IGBT
Input Harmonics	Fair (12-pulse) Poor (6-pulse) (6-p Thyristor)	Good (12-pulse) V Good (18pls)	Fair (12-pulse) Poor (6-pulse) (Thyristor Input)	Excellent
Input Power Factor (uncorrected)	Fair to Poor	Very Good	Fair to Poor (Thyristor Input)	Very Good
Output Harmonics	Poor	Good	Fair	Excellent
Output Common-mode Voltage	High (fair) (w/o Transformer)	None (excellent)	High (poor) (w/o Transformer)	None (excellent)
Output dV/dt (unfiltered)	High (poor)	Med-High (fair)	Low (good)	Low (good)
Regeneration Capability	Yes	No	Yes	No
Torque Pulsations	High (poor)	Low (very good)	Low (fair)	Virtually None (excellent)
Special Motor Required?	Yes, Synchronous	No	Yes (for common-mode voltage)	No
Speed Range (PU)	0.15 to 2.0	0 to 2.0	0 to 1.1	0 to 3.0
Special Starting Mode?	Yes	No	No	No

VFD Application Checklist

This section lists issues that should be considered in any VFD application. It is not meant to provide a detailed discussion, but rather to raise awareness on the part of the user or buyer as to necessary information and things to watch out for.

Line-Side Issues

1. What is the required motor power rating and the VFD input voltage and frequency?

- If the power rating is less than 500 kW, the use of a low-voltage VFD, i.e., 380 to 690 V rated input, should be considered. They are significantly cheaper then MV drives in the low power range.

- Oversizing the motor and VFD may lead to poorer harmonic and power factor performance of the VFD, as well as lower efficiency.

- Rated motor power is attained at its rated voltage and frequency. If the load reaches rated motor torque at less than rated speed, then rated power will not be delivered as the motor and VFD will have reached rated current, before rated voltage is attained. This can be a difficulty with pumping systems where the head is not exactly known. If the full torque is not attained until somewhat above rated frequency, then the VFD and motor can deliver rated power by operating in the constant power range.

2. What is the required tolerance on voltage and frequency?

- This especially applies to power systems that are fed by a generator, and may have more significant fluctuations.

- Typically, a VFD will be able to provide rated output within the range of 95 percent to 110 percent of nominal input voltage, with a plus or minus 5 percent tolerance on frequency.

- Some VFDs can produce less than rated output at significantly less than rated input voltage. VFD performance needs to be coordinated with the user's requirements.

3. Are there special requirements on ride-through? (Ride-through occurs when there is a utility line disturbance, e.g., a sag, swell, or transient, and the VFD continues to operate without tripping.) What happens if the drive trips and restarts on a line disturbance? Is such a condition acceptable to the driven load or process?

4. What is the input power factor (PF) requirement (either from the utility or the user)?

- Voltage-fed VFDs typically have a good PF at any load and speed without correction.

- Current-fed VFDs may require correction capacitors or an active front end.

5. What are the input harmonic current limits imposed by the utility or the user? IEEE 519 (1992) or other?

- What is the utility system impedance (short circuit current or MVA)? These data are needed to perform harmonic calculations. The VFD supplier can perform them, but needs to have valid source impedance data.

- Are there requirements for maximum voltage drop or flicker? Flicker is covered by IEEE 519 (1992) but is treated differently from harmonic distortion. This may be an issue for loads that fluctuate over a two to ten second range. It is not usually a problem with a pump or fan load.

- Is this an "islanded" supply, like an oil platform or water treatment plant on emergency power? If so, what are the characteristics of the generators and the power system impedance on which to base distortion calculations?

- What is the unbalance and distortion of the customer's utility? One needs to understand that a VFD's harmonic performance is adversely affected by preexisting distortion or unbalance. VFD manufacturers specify power factor and harmonics at the rated power of the VFD on the basis of an undistorted and balanced utility supply.

- Below 500 kW, there are situations in which a six-pulse input is acceptable, but above 1 MW, the minimum pulse number is 12, and 18 pulse or more may be needed in some cases.

- Using the same pulse number in a diode rectifier as compared to a thyristor rectifier does not give the same harmonic results. In the thyristor rectifier, the higher order harmonics are larger due to the higher di/dt values present in thyristor circuits.

6. Is there a requirement for input switch-gear with the VFD, such as a disconnect switch?

7. Is there a requirement for input protection instruments? Typically, VFDs have built in overcurrent protection on both line-side and machine-side, as well as undervoltage protection, but some users may want more functions.

8. Are there large utility power factor correction capacitors nearby?

- The drive may trip when they are switched on, due to the disturbance caused by connecting uncharged capacitors to the utility supply.

- For drives with significant input harmonics, the capacitors may resonate with the source inductance at a harmonic frequency. This creates large (undesirable) voltages at the harmonic frequency, and sometimes requires adding detuning reactors in series with the capacitors.

- Drive manufacturers always assume that there will be no power factor correction capacitors on the motor, as they may interfere with the drive operation. PF correction capacitors shall not be put on the output of a VFD!

- It is permissible to put surge capacitors on an MV motor fed by a VFD, but it is not necessary.

9. Is there a dedicated stepdown transformer feeding the VFD input? This is called a drive isolation transformer, or DIT. If so, the effect of the VFD input harmonics on the transformer must be considered.

- If there is a transformer integral to the VFD, or a DIT feeding the VFD, one should check to make sure that the user's utility can withstand the inrush of the transformer when it is energized. Saturation inrush events can be as large a 10 to 12 PU current.

Environmental and Physical Issues

1. Is there adequate space for the VFD or is space limited? If so, how? Medium-voltage VFDs are big due to the need for clearances inside.

2. What is the requirement for protection class of the VFD enclosure (e.g., IP22, NEMA 12, etc.)?

- The most common protection classes for VFDs are NEMA 1/IP22 (finger-proof and drip-proof), and NEMA 12/IP54, which is finger-proof, drip-proof, and dust-tight. These protection classes are not intended for outdoor applications, but must be placed in an indoor electrical room.

- For application requiring an outdoor location of the VFD, a special weatherproof enclosure is usually available in which the VFD is located and is equipped with ambient control.

3. What is the user's requirement for maximum ambient temperature and humidity?

- The industrial standard for maximum ambient is 104°F (40°C) and 95 percent relative humidity, noncondensing.

- Higher ambient temperatures can sometimes be accommodated by derating the current output of the VFD, if it is directly air-cooled.

4. What is the altitude of the installation? High altitudes require thermal derating and there is also a concern for the reduced dielectric strength of the air.

- A rule of thumb is to derate air-cooled equipment by 1 percent per every 328 ft (100 m) above 3281 ft (1000 m) altitude.

5. Are there corrosive gases present (like hydrogen sulfide, chlorine, ozone, etc.)? These are common in water-treatment plants, and all electronic equipment can be damaged by concentrations above a few parts per billion (ppb).

6. Is there conductive dust in the environment (e.g., coal dust)? Conductive dust will encroach on the creep spacing between live parts, and it must be kept out of the VFD and any electrical equipment.

7. Is the application at a seacoast environment? That location aggravates the humidity and corrosive gas conditions.

8. How will the drive losses be dissipated into the local environment? Modern VFDs are very efficient, and the larger the VFD, the more efficient.

- Typical efficiencies for VFDs above 1 MW are above 96 percent including the transformer (efficiency should not be a significant factor in choosing among different VFDs).

- Transformer losses must be considered in case of an indoor installation. Often, VFD manufacturers state efficiency without the transformer.

- Is there adequate cooling-air or air-conditioning for an air-cooled unit? The building has to be able to absorb the losses continuously, or draw in fresh air from outside and exhaust heated air.

- Large VFDs are frequently water-cooled with a deionized water loop inside. In that case, there is a water-to-water heat exchanger to user cooling water, or a water-to-air heat exchanger located outside.

9. Is the installation in a seismic zone that requires certification? If so which standards apply? Usually, as a minimum, foundation bolts must be designed to prevent the drive enclosure from toppling over due to the effect of lateral acceleration forces.

10. Are there shock and vibration requirements? Some VFDs are designed to withstand shock and vibration, but not all.

11. Is this a marine application aboard ship? If so, which standards apply? Some but not all VFDs are designed to marine standards, such as ABS and Lloyds.

12. Is there a customer requirement for acoustic noise?

13. What is the customer's requirement for efficiency?

- In evaluating efficiency, all the equipment associated with the VFD installation must be included. This includes power electronics, input transformer, input filters, output filters, and auxiliaries.

- The difference in efficiency among modern VFDs is very small compared to the energy savings to be attained by eliminating valves and dampers as a flow control method.

14. Is the VFD location a hazardous or potentially hazardous area (classified area per NEC)? VFD enclosures are almost never explosion-proof.

15. Does the VFD go into a mine, nuclear power plant or other strictly regulated location? There may be special standards and regulations that apply, which rule out standard VFD designs.

16. Is third-party certification required (like UL, CE, or CSA)? In some applications, local codes require such a certification for the VFD.

Machine-Side Issues

1. What is the rated motor power, voltage, full-load current, and frequency?

- The VFD has to have a current rating at least as large as the motor full-load amps.

- The motor has to be chosen for the required maximum torque, not power. Motor power is nominally defined at the base frequency and drops with speed.

2. Is extended speed operation required; what is the maximum frequency (extended speed is an operating regime above rated frequency where the voltage is held constant, but the frequency is increased)? This is an application issue for the motor, as they are not usually guaranteed to operate satisfactorily above rated speed, but they can be designed for such duty.

3. What are the motor parameters? Synchronous, induction, or wound rotor? The VFD manufacturer should be able to obtain the parameters to check for VFD motor compatibility.

4. Is the VFD going to be used with a motor that is smaller or larger than the VFD power rating? In some drives this creates a component sizing issue and the VFD manufacturer should be advised.

5. Is this a retrofit VFD onto an existing motor? Is the VFD compatible with an existing motor?

- Is the insulation system capable of handling the peak voltages?

- Is the insulation system capable of handling the dv/dt?

- Is the insulation system capable of handling common-mode voltage, i.e., voltage on the windings with respect to earth?

6. In case of a synchronous motor application

- In a synchronous motor, an excitation source is necessary for the motor field. This has to be considered in the design of the VFD.
- What kind of excitation is necessary?
  - Brush-type, brushless with DC stator exciter (common on motors for direct-on-line applications), or brushless with AC stator exciter
- Who is to supply the excitation power supply?
- What is the voltage and frequency of the auxiliary power supply that will feed the exciter power supply?
- Is this an LCI retrofit? In some cases load commutated inverters have become too old to be effectively supported, and may be replaced with a more modern drive without need to change the motor.

7. Is synchronous transfer required (In synchronous transfer, the VFD brings the motor up to the speed corresponding to the utility frequency, and phase synchronizes the motor voltages to the utility. Then there is a contactor that closes to connect the motor to the utility, after which the VFD contactor opens.)? If so, one needs to make sure that there is a supplier for the switch-gear and the master programmable logic controller (PLC) to coordinate the transfer.

8. What is the customer requirement for torque pulsations, if any? Some applications are very sensitive to torque pulsations as they may excite a shaft-train torsional natural frequency. In these cases, a special VFD may be necessary. The VFD manufacturer can describe the frequency and amplitude of torque pulsations for use in a torsional rotordynamic analysis.

9. Is this a single motor or multiple motor application? If different motors are to be used on a single drive (as in a test stand), the range of power and voltage needs to be specified. It can be difficult to tune a VFD for a wide range of motors.

10. Is there a stepup transformer on the output of the VFD? This presents special difficulties for the VFD and for the transformer.

- It is not a recommended configuration.
- What amount of starting torque is required? This is a key variable in designing the transformer.

11. Is this a long cable (over 3281 ft [1000 m]) application? Does the customer have a requirement for voltage distortion, dv/dt, and peak voltage at the motor? If so, what are the cable parameters and length?

12. Is there a customer requirement for distortion at the motor?

- The motor leakage inductance filters the voltage such that significantly less high-frequency current flows into the motor. Because of this there is more voltage distortion than current distortion.
- It is the distortion of the current that is important to the motor performance.

13. Is there a requirement for switch-gear between the VFD and the motor? It is important to assure that it is properly specified and that it is interlocked with the VFD.

- An output contactor should close before the VFD run request is issued.
- An output contactor should not open before the VFD has stopped passing current to the motor.
- In general, one should avoid opening contactors to operating power electronics so that current interruption transients are minimized.

14. Is there a requirement for motor/cable insulation system monitoring equipment? These systems may not work on VFDs. The partial discharge detection devices may not work either, due to the high frequency content of the VFD output.

15. Is there a requirement for motor protection instruments? Some commercially available motor protection instruments do not work except at 50 or 60 Hz.

16. Is the motor location a hazardous or potentially hazardous area (classified area)?

17. Bearing currents have been an issue in some LV motors and drives. The most conservative practice for MV VFD applications is to use an insulated bearing on the nondrive end, and apply a shaft grounding device on the drive end.

Load Issues

1. What is the speed-torque curve of the application? Is it a centrifugal load or constant torque, or something else? What is the normal operating speed range?

- This is important for the proper coordination of VFD, motor, and load. Motors are frequently self-cooled by means of an internal fan, and therefore cooling is less efficient at lower operating speeds.
- Centrifugal loads, in which the torque is proportional to the square of the speed, almost never require special cooling provisions in the motor.
- Constant torque loads, where the torque is a constant independent of speed, will need special cooling provisions at operating speeds less than 1 PU.
- The VFD is generally force-cooled by air or water, so it does not matter what kind of load is applied.

2. How much starting torque is required?

- All motors and rotating loads with sleeve bearings have a breakaway torque, which is the torque required to overcome the bearing friction when there is no oil film.
- Some applications require very large starting torque, such as SAG mills and conveyors. In these cases, extra current may be needed from the VFD to get the torque.
- Starting torque is a complicated issue because the drive controls do not work as well at zero speed. It needs to be considered that PU torque from the motor cannot be greater than the PU current supplying it. Of course it is always possible to get less if the control is incorrectly tuned.

3. Are there overloads applied? What is the peak overload torque, and the speed at which it is applied? How often does the overload occur?

- There are two kinds of overload ratings in the VFD world: 150 percent for one minute and 110 percent for one minute. The latter is used for easy to start loads (centrifugal), and the former for hard to start applications.
- The power electronic devices have to be sized to handle the peak value of current, as well as the average power losses. Therefore, a power electronics apparatus does not have the overload capacity of an electric machine or transformer.

4. Is there a gearbox in the drive train? The effect of pulsating torque may cause the gears to wear prematurely. In this case, one needs to be extra careful about torque pulsations and possible resonances.

5. Is the application a rapid pulsating load, such as a reciprocating compressor? If so, what is the torque versus crank angle curve? This may have an effect on VFD tuning and sizing.

6. Does this application require regeneration (regeneration is when the motor acts like a generator and continuously returns electrical energy to the VFD, taking it from the kinetic energy of the load. The energy is then returned to the utility source)? If so how much and for how long?

- Most voltage-source VFDs cannot regenerate energy to the utility.
- Some current-fed VFDs like LCIs can continuously regenerate.

7. Does this application require dynamic, occasional, or emergency braking? If so, how much and for how long (Dynamic braking is when the motor acts like a generator and continuously returns electrical energy to the VFD, taking it from the kinetic energy of the load. The energy is then dissipated in a resistor, and not returned to the utility.)?

- Some voltage-source VFDs can be equipped with a dynamic braking package that permits this kind of application.

8. Is this a cyclic load? What are the peak torques and duty cycles?

- Make sure that the rms current rating of the motor and VFD are not exceeded.

9. Does the customer require a special factory test regime, or a back-to-back test? These tests are time-consuming and expensive.

CONCLUSIONS

The application of VFDs in pumping applications provides the user with a number of benefits. However, large continuous VFD operating speed ranges greatly increase the risk of encountering resonance conditions of some kind. While centrifugal pump operating problems and failures can be caused by a variety of sources, only Resonance problems are directly related to VFD operation. The four resonance categories of concern are associated with lateral rotordynamics, torsional rotordynamics, structural dynamics, and acoustic resonance. Each of these categories has its own recommended analyses and checks (to identify resonances), detuning methods, and risks if not acted upon. Operation at lowly damped resonance conditions can result in excessive mechanical vibration and related failures. Table 6 summarizes the main phenomena, analysis methods and recommended corrective action in case of resonance. The preceding text should be consulted for more detailed and complete information. The appropriate set of analyses and checks can reliably replace a factory string-test aimed at identifying resonance conditions/ensuring acceptable vibration performance.

Table 6. Summary of Resonance Issues, Analyses, and Corrective Action.

Category		Excitation Mechanism & Frequency	Risks	Recommended Analyses & Checks	Corrective Action
Lateral Rotordyn.	Horizontal Pumps	1x (Unbalance)	Excessive lateral shaft vibrations 1.)	Lateral rotor analysis per API 610 8th or equivalent 2.)	See text for acceptance criteria, detuning methods and means to reduce excitation levels.
	Vertical Pumps	1x (Unbalance) 0.5x (Instability)	Excessive lateral shaft vibrations 1.) Excessive shaft- and structural vibr.	Combined lateral-structural analysis	Detune / avoid structural resonance excitable by 1x and 0.5x
Torsional Rotordyn.	Horizontal Pumps Vertical Pumps	Start-up, Short-circuit (Transient) VFD torque harmonics (Steady-state)	No risk, no analysis required because of VFD protection, slow start-characteristic of VFDs and low VFD torque harmonics (exception: LCI-VFDs)		No corrective action necessary.
Structural Dynamics	Horizontal Pumps	1x (Unbalance) Pressure pulsations at vane-pass frequency	1x: Baseplate resonance 3.) Vane-pass: High bearing housing vibrations	FEA of baseplate Impact test on bearing housings	Avoid / detune baseplate resonances Detune bearing housing resonances or reduce excitation levels 4.)
	Vertical Pumps	1x (Unbalance) 0.5x (Instability)	High vibration of partial- or full structure	FEA of structure	Application of seismic supports, detuning weight. Stiffening of components.
Acoustic Resonance (AR)	Horizontal Pumps Vertical Pumps	Pressure pulsations at vane-pass frequency	Long cross-over AR: Excessive bearing housing vibrations. Piping resonance: Excessive piping vibrations etc.	AR check if applicable	Avoid AR with vane-pass excitation frequency. See text for detuning methods and means to reduce excitation levels.

1. Excessive lateral shaft vibrations can cause mechanical seal failures, damage to journal bearing, touching/rubbing/wear in annular seals, high bearing housing vibrations (vibration transferred from shaft to journal bearing), noise, etc.

2. In case a fixed speed horizontal pump is converted to VFD operation, the existing fixed-speed lateral analysis may sufficiently cover the continuous VFD operating speed range. This needs to be carefully assessed on a case-by-case basis.

3. Baseplate resonance can cause excessive bearing housing and casing vibration. This could result in fatigue failures of piping, bolts, etc., as well as coupling failures.

4. Not all amplitude peaks revealed by impact testing represent excitable structural modes and the vane-pass excitation levels may be low, not resulting in excessive vibration levels (e.g., large B-gap, operation close to BEP, operation at low power levels).

NOMENCLATURE

A	= Area; ampere
c, c_1	= Speed of sound
c_u	= Circumferential fluid velocity
D	= Critical damping ratio (--)
D_A, D_B	= Pipe diameter
Da	= Annular seal diameter
D_3	= Volute lip diameter
D_2	= Impeller outer diameter
dv/dt	= Rate of rise of applied voltage
di/dt	= Rate of rise of applied current
E	= Young's modulus of elasticity
F	= Unbalance force ([lbf] or [N])
f	= Frequency (Hz)
G	= ISO balance quality grade (mm/sec)
K	= Balance constant
Kxx	= Stiffness
K_S	= Adiabatic (isentropic) bulk modulus
M, m	= Mass (kg)
N	= Rotor speed (rpm)
n	= Integer (--)
ΔP	= Pressure differential ([psi] or [Pa])
ΔP*	= Dimensionless pressure differential (--)
q*	= Normalized flow (--)
R	= Radius
s	= Slip
rms	= Root mean square
t	= Wall thickness; time (sec)
U	= Unbalance ([oz in] or [kg m])
Uxx	= Displacement
u_2	= Fluid velocity at impeller outlet ([ft/sec] or [m/sec])
V	= Volt
W	= Mass (lbm)
Z	= Acoustic impedance
z_2	= Impeller vane count (--)
Q	= Flow rate ([gpm] or [m^3/sec])
α_X	= Eigenvalue real-part
λ	= Eigenvalue (–); wavelength ([m] or [in])
ρ	= Density ([lb/ft^3] or [kg/m^3])
φ	= Phase (rad)
ω	= Angular speed of rotation (rad/sec)
ω_R	= Rotor angular velocity (rad/sec)
ω_S	= Stator flux angular velocity (rad/sec)
ω_x	= Angular natural frequency (rad/sec)

List of Acronyms

AC	= Alternating current
DC	= Direct current
DIT	= Drive isolation transformer

EMF = Electromagnetic field
GTO = Gate-turn-off (thyristor)
IGBT = Insulated gate bipolar transistor
IGCT = Integrated gate controlled thyristor
IM = Induction motor
kV = Kilovolts
kVAR = Kilovolt-amperes reactive
KW = Kilowatt
LSI = Large-scale integrated (circuit)
LCI = Load commutated inverter
LV = Low voltage
MCT = MOS controlled thyristor
MMF = Magnetomotive force
MOS = Metal-oxide semiconductor
MOSFET = Metal-oxide semiconductor field-effect transistor
MTO = MOS turn-off thyristor
MV = Medium voltage
MVA = Megavolt ampere
MW = Megawatt
NPC = Neutral point clamped
ppb = Parts per billion
PF = Power factor
PLC = Programmable logic controller
PU = Per unit (ratio of actual motor torque to rated (static) motor torque)
PWM = Pulse width modulation
RC = Resistor-capacitor
SCR = Silicon controlled rectifier
SGCT = Symmetrical gate controlled thyristor
WRIM = Wound-rotor induction motor
VFD = Variable frequency drive
VA = Voltage-ampere
VAC = Volts of alternating current
VAR = Voltampere reactive

REFERENCES

API Standard 610, Eighth Edition , 1995; Ninth Edition, 2003; Tenth Edition, 2004, "Centrifugal Pumps for Petroleum, Petrochemical and Natural Gas Industries," American Petroleum Institute, Washington, D.C..

Ewins, D. J., 1986, *Modal Testing: Theory and Practice,* Baldock, England: Research Studies Press.

Guelich, J. F. and Bolleter, U., 1992, "Pressure Pulsations in Centrifugal Pumps," ASME Journal *Vibration Acoustics*.

Guelich, J. F. and Egger, R., March 1992, "Part Load Flow and Hydraulic Stability of Centrifugal Pumps," EPRI report TR-100219.

IEEE Standard 519, 1992, "Recommended Practices and Requirements for Harmonic Control in Electrical Power Systems," The Institute for Electrical and Electronic Engineers, Piscataway New Jersey.

IRD Balancing Technical Paper 1, 2007, "Balance Quality Requirements of Rigid Rotors—The Practical Application of ISO 1940/1," Entek IRD Balancing, Columbus, Ohio.

ISO Standard 13709, 2003, "Centrifugal Pumps for Petroleum, Petrochemical and Natural Gas Industries," International Organization for Standardization, Geneva, Switzerland.

Richardson, M. H., March 1997, "Is it Mode Shape, or an Operating Deflection Shape?" *Sound and Vibration Magazine,* Bay Village, Ohio.

BIBLIOGRAPHY

API Standard 684, 1999, "Tutorial on the API Standard Paragraphs Covering Rotor Dynamics and Balancing: An Introduction to: Lateral Critical and Train Torsional Analysis and Rotor Balancing," First Edition, American Petroleum Institute, Washington, D.C.

ANSI/HI Standard 2.1 2.5, 1994, "American National Standard for Vertical Pumps—For Nomenclature, Definitions, Applications and Operation," Hydraulic Institute, Parsippany, New Jersey.

Bedford, B. D. and Hoft, R. G., 1964, *Principles of Inverter Circuits,* New York, New York: John Wiley & Sons, (ISBN-10: 0471061344).

Bose, B. K., 1981, *Adjustable Speed AC Drive Systems,* New York, New York: John Wiley & Sons.

Brichant, F., 1984, *Force-Commutated Inverters,* New York, New York: McGraw-Hill Publishing Company (ISBN-10: 0070077134).

Cornman, R. E., 1986, "Analytical and Experimental Techniques for Solving Pump Structural Resonance Problems," *Third International Pump Users Symposium,* Turbomachinery Laboratory, Texas A&M University, College Station, Texas, pp. 27-32.

Dickau, R. and Pardo, C., 2004, "Centrifugal Pumps in Heated Bitumen Pipeline Service," *Twenty-First International Pump Users Symposium,* Turbomachinery Laboratory, Texas A&M University, College Station, Texas, pp.10-17.

Ehrich, F. F., 1992, *Handbook of Rotordynamics,* New York, New York: McGraw-Hill Publishing Company (ISBN 0-07-019330-4).

Europump, May 2004, "Variable Speed Pumping—A Guide To Successful Applications," Brussels, Belgium.

Graff, K. F., 1975, *Wave Motion in Elastic Solids,* New York, New York: Dover Publications (ISBN 0-486-66745-6).

Ghandi, S. K., 1977, *Semiconductor Power Devices,* New York, New York: John K. Wiley & Sons.

Guelich, J. F., 1999, *Kreiselpumpen—Ein Handbuch fuer Entwicklung, Anlagenbau und Betrieb,* Berlin, Germany: Springer-Verlag.

IEC Standard 60529, 1999, "Degrees of Protection Provided by Enclosures (IP Code)", Edition 2.1.

Kosow, I. L., 1973, *Control of Electric Machines,* Englewood Cliffs, New Jersey: Prentice-Hall.

Lienau, W., 2005, "Identification of Bearing Housing Vibrations of a Large Barrel Type Injection Pump and Their Analysis by Means of the Finite Element Method," *Twenty-Second International Pump Users Symposium,* Turbomachinery Laboratory, Texas A&M University, College Station, Texas, pp. 1-9.

Marks' Standard Handbook for Mechanical Engineers, Tenth Edition, 1996, E. A. Avallone, T. Baumeister III, Editors, New York, New York: McGraw Hill (ISBN 0-07-004997-1).

Marscher, W. D. and Campbell J. S., 1998, "Methods of Investigation and Solution of Stress, Vibration, and Noise Problems in Pumps," *Fifteenth International Pump Users Symposium,* Turbomachinery Laboratory, Texas A&M University, College Station, Texas, pp. 143-156.

NEMA Standards Publication 250, 1997, "Enclosures for Electrical Equipment," National Electrical Manufacturers Association, Rosslyn, Virginia.

Pelly, B. R., 1971, *Thyristor Phase-Controlled Converters and Cycloconverters,* New York, New York: John K. Wiley & Sons.

Rao, S. S., 1995, *Mechanical Vibrations,* Third Edition, Addison-Wesley Publishing Company (ISBN 0-201-52686-7).

Robinett, F. L., Guelich, J. F., and Kaiser, T., 1999, "Vane Pass Vibration—Source, Assessment, and Correction—A Practical Guide for Centrifugal Pumps," *Sixteenth International Pump Users Symposium,* Turbomachinery Laboratory, Texas A&M University, College Station, Texas, pp. 121-138.

Schaefer, J., 1965, *Rectifier Circuits: Theory and Design,* New York, New York: John K. Wiley & Sons.

Schwartz, R. E. and Nelson R. M., 1984, *"Acoustic Resonance Phenomena in High Energy Variable Speed Centrifugal Pumps," First International Pump Symposium,* Turbomachinery Laboratory, Texas A&M University, College Station, Texas, pp. 23-28.

Scoles, G. J., 1981, *Handbook of Rectifier Circuits,* New York, New York: John K. Wiley & Sons.

Sen, P. C., 1981, *Thyristor DC Drives,* New York, New York: John K. Wiley & Sons.

Vance, J. M., 1988, *Rotordynamics of Turbomachinery,* New York, New York: John K. Wiley & Sons (ISBN 0-471-80258-1).

ACKNOWLEDGEMENTS

The authors would like to thank the managements of Sulzer Pumps Inc. and Siemens Energy & Automation Inc. for permission to publish this paper.